Scientific African 33 (2026) e03514

Contents lists available at ScienceDirect

Scientific African

journal homepage: www.elsevier.com/locate/sciaf

Assessment of cyanide contamination in artisanal gold mining: a case study of Busia gold fields, eastern uganda

Denis Musiige [a,b,*], Jhonnah Mundike [a], Cuthbert Makondo [a]

[a] The Copperbelt University, School of Mines and Mineral Sciences, Environmental Engineering Department, P.O. Box 21692, Kitwe, Zambia
[b] The Copperbelt University, School of Postgraduate Studies, P.O. Box 21692, Kitwe, Zambia

ARTICLE INFO

Editor: Mohamed Fathy El-Amin Mousa

Keywords:
Environmental contamination
Seasonal variability
Ecological risk
Toxicity
Tailings

ABSTRACT

Artisanal and small-scale gold mining (ASGM) in Busia, Uganda, relies on cyanide for gold extraction. However, data on its environmental fate remain scarce, with most research focused on mercury. This study presents a systematic assessment of cyanide speciation across multiple environmental matrices at the Busia Gold Fields site. These included seepage water, surface water, waste water through pipes and trenches, sediments, and tailings, which were sampled comprehensively during the dry and wet seasons. Water and solid samples ($n = 140$) were analyzed for their physicochemical properties. The concentration of free cyanide (CN_{Free}), Weakly Acid Dissociable Cyanide (CN_{WAD}), Strongly Acid Dissociable Cyanide (CN_{SAD}), and Total Cyanide (CN_T) was determined using APHA-standard spectrophotometric techniques. Trench wastewater recorded the highest CN_{Free} (15.50 mg/L). Metallic pipe drainage exhibited the most extreme conditions (pH 3.07–3.78; EC up to 11,800 μS/cm). Seepage and surface water yielded CN_T of 0.37–0.88 mg/L and 0.16–0.42 mg/L, respectively. Stream sediments accumulated CN_{SAD} up to 84.26 mg/kg, and sand-active tailings CN_T up to 79.09 mg/kg. Significant dry-to-wet seasonal reductions in CN_{Free} (34.8–49.5%, $p < 0.001$) were observed across all compartments but failed to achieve compliance with any applicable threshold. The majority of samples exceeded multiple regulatory thresholds. All 60 water samples surpassed the Uganda NEMA effluent standard and the WHO/FAO irrigation guideline. Out of 60, 55 exceeded the US EPA criterion, and 43 out of 60 exceeded the WHO short-term guideline. Wet-season seepage and surface water predominantly accounted for non-exceedances. Spearman correlation, two-way ANOVA, and principal component analysis confirmed that physicochemical gradients, particularly Eh, pH, and EC, governed cyanide speciation and mobility. Contrasting pH–CN_{Free} relationships between sediments ($\rho = -0.954$) and tailings ($\rho = 0.701$) captured the mechanistic duality between Acid Mine Drainage (AMD)-driven accumulation and alkaline cyanidation stabilization. These findings underscore the urgent need for source-specific remediation and integration of multi-fraction cyanide monitoring into Uganda's environmental regulatory framework.

Introduction

The economic advancement of countries relies on mining activities, especially in resource-rich regions such as Uganda [1]. Found

* Corresponding author at: The Copperbelt University, School of Mines and Mineral Sciences, Environmental Engineering Department, P.O Box 21692, Kitwe, Zambia.

E-mail address: musiigedenis81@gmail.com (D. Musiige).

https://doi.org/10.1016/j.sciaf.2026.e03514
Received 9 August 2025; Received in revised form 26 March 2026; Accepted 11 July 2026
Available online 11 July 2026
2468-2276/© 2026 The Author(s). Published by Elsevier B.V. This is an open access article under the CC BY-NC-ND license (http://creativecommons.org/licenses/by-nc-nd/4.0/).

within the East African plate, Uganda boasts a multitude of mineral resources, including beryl, bismuth, copper-cobalt, and gold [2]. The country's economy receives a substantial boost from gold mining operations, which have become one of its major economic contributors. The three central mining districts of Busia, Mubende, and Karamoja function as the primary areas of gold extraction, according to Nyakecho & Hagemann [3]. The artisanal and small-scale gold mining (ASGM) sector in Uganda contributes 3.5% to the country's Gross Domestic Product (GDP). About 200,000 people work in the gold mining sector across Uganda, as it produces 2.8 tons of gold per year [4]. The economic value of gold mining contrasts with significant environmental hazards and health threats. Harmful substances, including mercury, cyanide, and toxic waste products from the sector, contribute to this environmental damage [5].

Busia gold fields, a key site for artisanal and industrial gold mining, pose significant environmental and health risks, primarily due to cyanide pollution [6]. Ore extraction generates large quantities of tailings containing cyanide, mercury, and arsenic [7,8]. Improper handling of tailings and cyanide use in leaching threatens soil, water, and air quality, as well as biodiversity and local communities [9]. Cyanidation, first implemented in 1899, remains the predominant method for gold recovery due to stable $Au(CN)_2^-$ complex formation [10,11]. However, it produces cyanide-laden waste that, if unmanaged, presents enduring environmental hazards. Despite being an efficient ore-processing technique, cyanidation in ASGM is often practiced informally, with small-batch reprocessing, limited containment, and co-use with mercury. Such conditions heighten risks of uncontrolled releases from circuits and tailings [12]. In Uganda, miners frequently reprocess legacy tailings using inexpensive cyanide reagents and rudimentary equipment. This promotes direct discharge to soils and waters as well as formation of persistent metal–cyanide complexes. Although policy frameworks exist (Mining and Minerals Act; effluent standards), oversight and sector formalization remain weak [13,14]. Similar patterns are reported globally, where cyanide complements mercury processing and accumulates as free, weak-acid-dissociable, and firmly bound species in waters, sediments, and tailings [15,16]. This underscores the need to integrate monitoring with policy and best-practice management, such as the International Cyanide Management Code.

Gold mine tailings constitute residual cyanide and various hazardous components. These can dissolve into the surrounding environments, affecting the local soil and water supplies [17]. Open-pit mining and heap leaching generate large amounts of waste and cause contamination by potentially toxic elements (PTEs) [18–20]. Research findings show that about 90% of processed ore becomes waste materials [11]. Three different forms of cyanide exist in tailings: free cyanide (CN^-, HCN). This is a weak acid and can dissociate as ($HCN_{(aq)} \leftrightarrow H^+ + CN^-$) at a pH 6.0. Weak acid dissociable (WAD) cyanide (Copper, Zinc, Cadmium, Mercury, Nickel, and Silver complexes). These can dissociate at mildly acidic conditions at a pH 4 – 6, such as $Cu\ (CN)_3^{2-}$, $Zn\ (CN)_4^{2-}$, $Ni\ (CN)_4^{2-}$, and $Cd\ (CN)_4^{2-}$. Strong acid dissociable (SAD) cyanide includes Platinum, Gold, Iron, and Cobalt complexes. These requires strongly acidic conditions to dissociate, pH<2, such as $Pt\ (CN)_4^{2-}$, $Fe\ (CN)_6^{4-}$, $Au\ (CN)_2^{-}$, and $Co\ (CN)_6^{3-}$. SAD cyanide forms highly stable complexes with iron and gold [10]. Cyanide's fate in tailings is strongly influenced by pH, temperature, microbial activity, and oxidative processes. It is partially transformed into volatile HCN and metal–cyanide complexes, which generate toxic by-products in aquatic systems [21]. Such contamination causes fish mortality, biodiversity loss, and groundwater pollution [11]. In Busia's artisanal and small-scale gold mining (ASGM) sites, cyanide management is inadequate. They rely on presumed natural attenuation via volatilization, adsorption, UV degradation, and microbial oxidation to thiocyanate [22,23]. These processes are highly site-specific and insufficient without containment, resulting in persistent soil and groundwater contamination, food-safety threats, and public health risks [10].

Previous studies have shown that cyanide leakage from gold mine tailings contaminates nearby water bodies [23–26]. This affects both human populations and aquatic ecosystems [21]. The slow degradation of cyanide through volatilization and microbial activity does not eliminate its significant environmental risk when tailings are poorly managed [11]. Despite extensive documentation of mercury in Ugandan ASGM, evidence on cyanide quantities remains limited. Specific cyanide species across environmental compartments are scarcely characterized in active gold processing landscapes. The level of toxicity of cyanide varies markedly with concentration and speciation. CN_{Free} is acutely lethal at low μg/L levels while CN_{SAD} persists as a long-term reservoir in sediments and tailings. This makes multi-fraction speciation assessment essential for understanding environmental dynamics, exposure pathways, and regulatory compliance. In light of these critical knowledge gaps, this study presents a comprehensive, multi-compartment, two-season assessment of cyanide speciation at Busia Gold Fields, Uganda. Specifically, the research set out to: (i) quantify concentrations of CN_{Free}, CN_{WAD}, CN_{SAD}, and CN_T across seepage water, surface water, plastic pipe, trench and metallic pipe wastewater, stream sediments, and tailings dumps; (ii) examine spatial distribution and temporal variation of cyanide contamination across active and abandoned mining facilities; (iii) evaluate physicochemical controls governing cyanide speciation, mobility, and persistence across environmental matrices; and (iv) provide evidence-based insights for source-specific remediation, regulatory strengthening, and sustainable cyanide waste management in ASGM settings. In line with these objectives, the study was guided by the following testable hypotheses: H_1: Cyanide species concentrations differ significantly among environmental compartments and between seasons. H_2: Physicochemical parameters, particularly pH, redox potential (Eh), and electrical conductivity (EC), significantly govern cyanide speciation and mobility across matrices. H_3: Active and abandoned artisanal mining facilities exhibit statistically distinct cyanide contamination profiles. H_4: Cyanide concentrations at Busia Gold Fields exceed national and international environmental quality benchmarks.

Materials and methods

Study area

Busia District, located in eastern Uganda near the Kenyan border, lies between 33°05′E, 00°10′N and 34°01′E, 00°35′N as shown in Fig. 1. According to Mbonimpa et al. [24] and Omara et al. [6], the district occupies a total area of 731 km². The administrative district

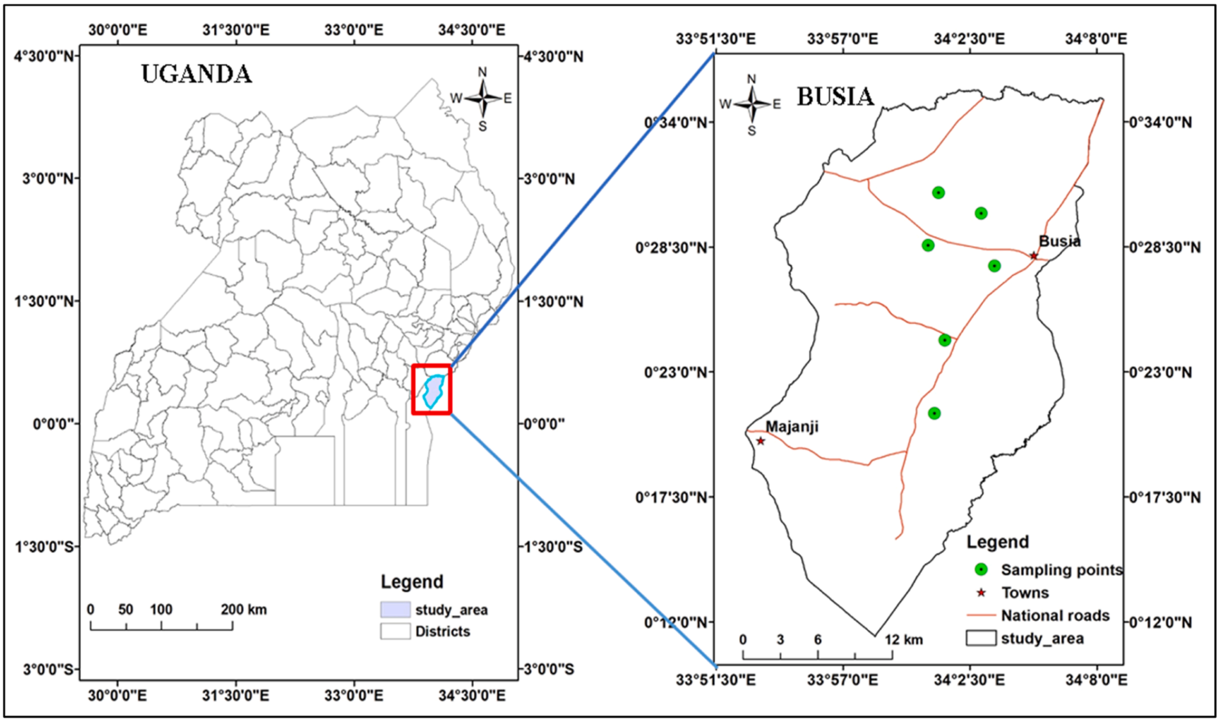

Fig. 1. Map showing the study area and locations of sampling points.

of Tororo separates Busia from Bugiri along its northwest border. Namayingo divides it from the west side, and Busia County, Kenya, stands as its eastern boundary [24]. From Kampala, the capital, the district is approximately 220 km to the east. Residents of the area mainly participate in agricultural work, commercial activities, and fishery operations whilst conducting artisanal gold mining [6]. Bordering four other districts, Busia is separated from Kenya by the Malaba River, while the Nanguke River flows through its interior [4].

Busia has a tropical rainforest climate, characterized by distinct wet and dry seasons. It receives two rainy seasons: one from March to May and another from October to November. The dry season spans from December to February and from June to September. The district receives an annual rainfall of 1200–1500 mm, with temperatures ranging from 18 to 32 °C throughout the year. Busia District is situated at a median elevation of 1158 m above sea level [27].

Sampling strategy, sample collection, and preparation

Sampling design

Sampling followed a stratified source–pathway–sink framework to capture (i) Cyanide primary sources (processing effluents and tailing dumps), (ii) transport pathways (seepage and surface water), and (iii) receiving sinks (stream sediments and wetland zones). To resolve both spatial and temporal variability, all matrices were sampled across two climatically contrasting seasons, that is, dry (June, 2025) and wet (March 2026). Dry-season sampling established the spatial framework. Wet-season resampling was conducted at GPS-verified locations identical to those of the dry season. This enables paired temporal comparisons free of spatial confounding. All sites were georeferenced using a Garmin GPSMAP 64sx and mapped in ArcGIS Pro 3.4 (ESRI, USA). A priori power analysis (one-way ANOVA, $k = 5$ water compartments, Cohen's $f = 0.40$, $\alpha = 0.05$, power = 0.80) determined minimum sample requirements of 12 per water compartment and 20 per solid-matrix stratum across both seasons. It yielded a study-wide total of 140 samples: 60 water samples, 40 stream sediment samples, and 40 tailings.

Water sample collection

Water sampling covered five operationally distinct compartments: seepage water, surface water, plastic pipe wastewater, trench wastewater, and metallic pipe wastewater. Six independent samples were collected per compartment per season, giving 12 per compartment and 60 water samples in total (30 per season). Seepage water (SW-D1–D6; SW-W1–W6) was sampled at shallow discharge points along base, mid-slope, and crest drainage zones. This approach underscores the critical role of seepage as the primary pathway for cyanide transfer from tailings into surrounding hydrological systems. Each seepage sample comprised three 500 mL composite subsamples collected within a 2 m radius and homogenized into a single analytical unit. Surface water (SS-D1–D6; SS-W1–W6) was collected at six stations along the principal stream, two upstream reference stations (≥ 500 m above mining influence), one mid-stream station at the first visible effluent input, and three downstream stations at 100 m intervals below the primary discharge

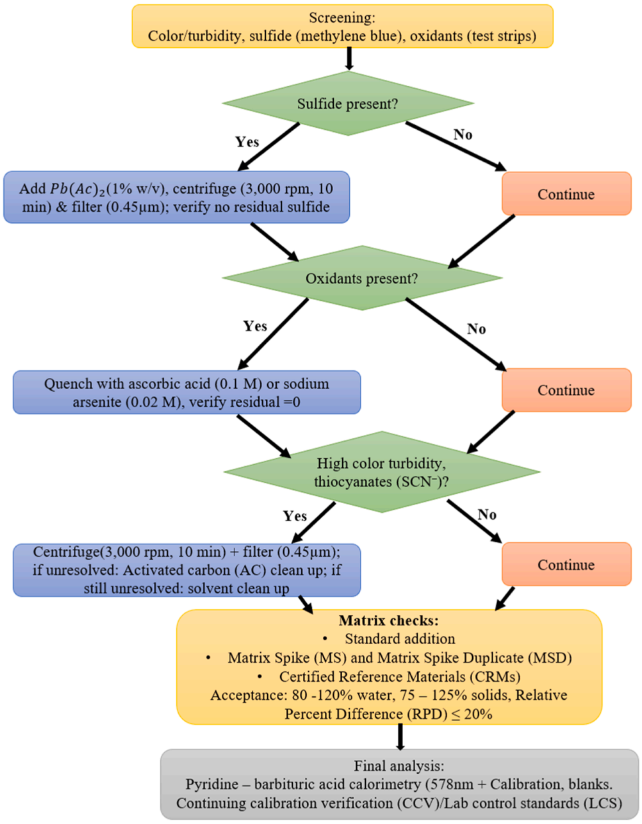

Fig. 2. Flowchart of the interference controls and matrix checks workflow.

zone. Wastewaters from plastic pipe (PP-D1–D6; PP-W1–W6), trench (TR-D1–D6; TR-W1–W6), and metallic pipe (MP-D1–D6; MP-W1–W6) were sampled at six distinct discharge points. They represented different operators, processing stages, or trench positions to capture within-compartment heterogeneity.

All samples were collected into High-Density Polyethylene/Polypropylene (HDPE/PP) bottles pre-soaked in 10% HNO_3 for 24 h. They were triple-rinsed with deionized water and given a final site-water rinse. Immediately upon collection, pH was raised to ≥ 12 with 6 N NaOH. This was verified using a calibrated BT-600 pH meter (BOECO, Germany) to prevent HCN volatilization and cyanide transformation during transport. Bottles were filled to zero headspace, sealed, and stored at approximately 4 °C in opaque insulated coolers. They were logged on chain-of-custody forms and transported to the laboratory within 24 h. Analyses were initiated within 14 days of collection per APHA 4500-CN-B preservation requirements. Field physicochemical parameters, including pH, temperature, redox potential (Eh), and electrical conductivity (EC), were measured in situ using calibrated instruments (BT-600 pH meter; CM-230 conductivity meter, BOECO, Germany; certified digital thermometer).

Stream sediment and tailings sample collection

Stream sediments (40 total; 20 per season) were collected across three spatially defined strata. Proximal ($\leq$ 100 m from active mining; n = 7 per season: MD-P1–P7; MW-P1–P7), mid-gradient (100–500 m downstream; n = 7: MD-M1–M7; MW-M1–M7), and distal/reference (> 500 m; n = 6: MD-D1–D6; MW-D1–D6). At each site, 500 g of sediment was collected from approximately 30 cm depth using a stainless-steel auger following removal of the surface oxidized layer (~5 cm). Three subsamples within a 5 m radius were homogenized in a clean polyethylene tray and transferred to black polyethylene bags to prevent photodegradation during transport.

Tailings (40 total; 20 per season) were collected across four strata defined by type and operational status. Conventional active (n = 5: AD-CA1–CA5; AW-CA1–CA5), conventional abandoned (n = 5: AD-CB1–CB5; AW-CB1–CB5), sand active (n = 5: AD-SA1–SA5; AD-SA1–SA5), and sand abandoned (n = 5: AD-SB1–SB5; AW-SB1–SB5). Surface material was collected by shovel to a depth of 10–15 cm; at abandoned dumps, an auger was used below the oxidized layer (15–30 cm). Five subsamples at the corners and center of a 4 m × 4 m grid were composited into a single 500 g analytical unit.

Sediment and tailings extraction for cyanide analysis

All solid samples (stream sediments, tailings) were homogenized upon arrival at the laboratory. Subsamples (50 g) were oven-dried at 105 °C to constant weight to determine moisture content (%), calculated as in equation (i):

Table 1
Quality assurance, method validation, and analytical performance parameters for spectrophotometric cyanide determinations.

No.	Subsection	Key details
1	Analytical method	Pyridine–barbituric acid spectrophotometric method, absorbance at 578 nm. Instrument: A Shimadzu UV-1280 spectrophotometer (Shimadzu, Japan). (Instrument settings in lab log).
2	Calibration & linearity	NaCN standards (0.01–2.00 mg L^{-1}; points: 0.01, 0.05, 0.10, 0.50, 1.00, 2.00). ≥ 5 non-zero points per curve. Linear regression (absorbance vs concentration), R^2 reported. Mid-level checks every 10 samples (±10% acceptance)—fresh curve when check failed.
3	Detection limits (EPA MDL procedure)	Low-level spike (1–5 × expected MDL), n ≥ 7 replicates with Method Detection Limit expressed as in equation (iii). $$MDL = t_{(n-1,\ 0.99)} \times s \quad \text{(iii)}$$ For n = 7, t ≈ 3.14. LOQ = 10 × s Determined for CN_{Free}, CN_{WAD}, CN_T using matrix-appropriate spikes.
4	Blanks & duplicates	Method, reagent, and field blanks: 1 per ≤10 samples. Duplicates: 1 per ~10 samples. Criteria: blanks< MDL; duplicate RSD ≤ 20% (≤15% for water >LOQ). Standards read in triplicate.
5	Matrix spikes & recovery	Water spikes: 0.05, 0.5 mg L^{-1}; solids: 1–10 mg kg^{-1}. MS/MSD frequency: 1 set per 10 samples. $$\%\text{Recovery} = \frac{\text{Measured spike} - \text{Native concentration}}{\text{Spike added}} \times 100. \quad \text{(iv)}$$ Acceptance: 80–120% (water), 75–125% (solids). Out-of-range → reanalysis.
6	Interference control	Sulfides removed with lead acetate, oxidants neutralized (sodium arsenite/ascorbic acid), particulates filtered (0.45 μm), thiocyanate quantified (Ion chromatography/colorimetry) to track CN transformation, standard-addition checks (NaCN spikes) verified matrix recoveries (80–120% water; 75–125% solids); preservation: pH ≥12 (CN_{Free}), adjusted for WAD distillations. Procedures per Standard Methods/EPA [33].
7	IPR & ongoing QC	IPR: replicate standards (n = 4), %Recovery & %RSD recorded. Ongoing: lab control standards (LCS) + continuing calibration verification (CCV); Acceptance ±15%. Failures → recalibration/reanalysis.
8	Uncertainty estimation	Components: calibration (u_{cal}) derived from regression, repeatability (u_{rep}) from duplicate analyses, and preparation (u_{prep}) from repeated extractions/spikes as in equation (v): $$u_c = \sqrt{u_{cal}^2 + u_{rep}^2 + u_{prep}^2} \quad \text{(v)}$$ Expanded uncertainty (95%): U = $k \times u_c$ with $k = 2$. Results reported as mean ± U (or mean ± SD, n shown).
9	Solids: MDL/LOQ conversion	$$MDL_{solid}(mgkg^{-1}) = \frac{MDL_{solution}(mgL^{-1}) \times V_{final}(L) \times 1000}{m_{sample}(g)} \quad \text{(vi)}$$ Where V_{final} = final extract volume, m_{sample} = solid mass analyzed.
10	References	Standard Methods 4500-CN, EPA SW-846 method 9013A, EPA 335.4, EPA MDL821-R–16–006 [28,29,34,35].

MDL: Method Detection Limit, **LOQ:** Limit of Quantification, **s:** Standard Deviation, **RSD:** Relative Standard Deviation, **RPD:** Relative Percent Difference, **IPR:** Initial Precision and Recovery, **QA:** Quality Assurance, **QC:** Quality Control, **EPA:** United States Environmental Protection Agency, **MS/MSD:** Matrix spikes/ Matrix spike duplicates. **U:** Uncertainty estimation.

$$Moisture\ \% = \frac{m_{wet} - m_{dry}}{m_{wet}} \times 100. \quad \text{(i)}$$

Cyanide concentrations in solids are reported on a dry-weight basis using equation (ii):

$$C_{dry}(mg/kg^{-1}) = \frac{C_{extract}(mg/L^{-1}) \times V_{extract}(L)}{m_{dry}(g)} \times 1000 \quad \text{(ii)}$$

where $C_{extract}$ is the analyte concentration in the aqueous extract, $V_{extract}$, the extract volume, m_{dry}, the dry sample mass, and m_{wet}, the wet sample mass.

The extraction and fractionation were done according to the procedure adapted from Standard Methods 4500-CN, EPA SW-846 [28,29]. Briefly, 25 g of homogenized sediment/tailings was placed in a 500 mL vessel with 250 mL deionized water (solid: liquid = 1:10). The sealed vessel was shaken end-over-end for 60 min at 20 – 25 °C and centrifuged at 3000 rpm for 10 min. The supernatant was filtered (0.45 μm). The resulting aqueous extract was used for CN_{Free} and CN_{WAD} determination.

Cyanide analysis

CN_{Free}, CN_{WAD}, and CN_T were determined spectrophotometrically using the pyridine-barbituric acid colorimetric finish at 578 nm on a Shimadzu UV-1280 spectrophotometer (Shimadzu, Japan). Samples were preserved at pH ≥ 12 with 6 N NaOH, stored at 4 °C, and analyzed within 14 days of collection.

Free cyanide (CN_{Free}) was determined by direct colorimetry following APHA 4500-CN-E [28]. A 50 mL aliquot was filtered through a 0.45 μm cellulose nitrate membrane; 10 mL of the filtrate was reacted with 0.5% w/v chloramine-T (2 mL, 2 min) to generate cyanogen chloride, followed by the addition of pyridine-barbituric acid reagent (5 mL). Colour was developed for 8 min at 20–25 °C, and absorbance was measured at 578 nm. pH was maintained below 8 throughout to prevent hydrolysis of cyanogen chloride to cyanate. Calibration employed NaCN standards over 0.01–2.00 mg CN^- L^{-1}.

Table 2
Quality assurance, method validation, and analytical performance data for spectrophotometric cyanide analysis (pyridine–barbituric acid method).

No.	Analyte (fraction)	Matrix	Calibration range (mg L^{-1})	Calibration equation $y = mx + b$	R^2	MDL (mg L^{-1})	LOQ (mg L^{-1})	Method blank (mg L^{-1})	Spike Recovery (%) ± SD	RSD (%)	CRM / Check Standard (Found / Certified mg L^{-1})	comment
1	Free cyanide (CNFree)	Water	0.01–2.00	$y = 0.345x + 0.002$	0.999	0.002	0.007	<0.002	99 ± 4.0	4.2	0.096 / 0.100	Triplicate water replicates; blank below MDL.
2	Weak acid dissociable (CNWAD)	Water	0.02–2.00	$y = 0.298x + 0.004$	0.998	0.005	0.015	<0.005	98 ± 5.0	5.6	0.47 / 0.50	Spikes (0.05 & 0.50 mg L^{-1}); recoveries acceptable.
3	Total cyanide (CNT)	Water & solids	0.01–2.50	$y = 0.325x + 0.003$	0.999	0.003	0.010	<0.003	100 ± 5.0	6.3	0.048 / 0.050	Calibration and CCV within ±10%.

MDL and **LOQ** were calculated as 3σ and 10σ of replicate blank measurements (n = 10). Spike recoveries based on matrix-matched fortifications at 0.05–2 mg L^{-1} (± SD from triplicates).
CRM verification performed using ERA WP Cyanide, Sigma Trace CERT, BAM Soil, and NIST SRM 1643f standards. All instrumental RSD values< 10%, indicating excellent precision and stability across matrices.

Table 3
Physicochemical characteristics and concentration (mg/L) of cyanide species for seepage and surface water samples in the dry and wet seasons.

Sample	Temp (°C)	pH	EC (μS/cm)	Eh (mV)	CN_{Free}	CN_{WAD}	CN_{SAD}	CN_T
Seepage water — Dry season, n = 6								
SW-D1	10.90	6.58	510	257	0.29	0.32	0.37	0.69
SW-D2	12.60	6.82	500	270	0.31	0.33	0.45	0.78
SW-D3	11.40	6.71	525	263	0.34	0.36	0.46	0.82
SW-D4	13.10	6.90	542	281	0.37	0.38	0.50	0.88
SW-D5	11.80	6.65	518	268	0.30	0.34	0.41	0.75
SW-D6	12.20	6.74	532	275	0.33	0.35	0.45	0.80
Mean ± SD	12.00 ± 0.80	6.73 ± 0.12	521 ± 15	269 ± 9	0.32 ± 0.03	0.35 ± 0.02	0.44 ± 0.04	0.79 ± 0.06
Seepage water — Wet season, n = 6								
SW-W1	14.20	6.32	380	241	0.18	0.21	0.25	0.46
SW-W2	15.10	6.18	362	228	0.15	0.19	0.22	0.41
SW-W3	13.80	6.41	395	252	0.21	0.23	0.29	0.52
SW-W4	14.60	6.24	371	235	0.17	0.20	0.24	0.44
SW-W5	15.40	6.09	348	219	0.13	0.17	0.20	0.37
SW-W6	14.90	6.15	358	226	0.14	0.18	0.22	0.40
Mean ± SD	14.67 ± 0.59	6.23 ± 0.12	369 ± 17	234 ± 12	0.16 ± 0.03	0.20 ± 0.02	0.24 ± 0.03	0.43 ± 0.05
Surface water — Dry season, n = 6 (2 upstream, 1 mid-stream, 3 downstream)								
SS-D1(up)	11.90	6.64	420	316	0.06	0.08	0.08	0.16
SS-D2(up)	14.80	6.56	490	274	0.14	0.13	0.11	0.24
SS-D3(mid)	13.50	5.42	640	398	0.09	0.14	0.14	0.28
SS-D4(dn)	15.40	4.36	860	485	0.03	0.16	0.05	0.21
SS-D5(dn)	16.00	4.24	920	502	0.14	0.22	0.20	0.42
SS-D6(dn)	15.70	4.31	892	494	0.11	0.19	0.17	0.36
Mean ± SD	14.55 ± 1.57	5.25 ± 1.13	704 ± 218	412 ± 99	0.10 ± 0.04	0.15 ± 0.05	0.13 ± 0.06	0.28 ± 0.10
Surface water — Wet season, n = 6 (2 upstream, 1 mid-stream, 3 downstream)								
SS-W1(up)	16.80	6.48	310	289	0.04	0.06	0.06	0.12
SS-W2(up)	17.20	6.41	295	274	0.05	0.07	0.07	0.14
SS-W3(mid)	17.90	5.18	480	362	0.06	0.11	0.09	0.20
SS-W4(dn)	18.40	4.52	620	441	0.02	0.10	0.06	0.16
SS-W5(dn)	18.90	4.41	672	458	0.08	0.14	0.14	0.28
SS-W6(dn2)	18.60	4.47	648	450	0.05	0.12	0.10	0.22
Mean ± SD	17.97 ± 0.83	5.25 ± 0.97	504 ± 170	379 ± 83	0.05 ± 0.02	0.10 ± 0.03	0.09 ± 0.03	0.19 ± 0.06

Weak acid dissociable cyanide (CN_{WAD}) was determined by acid distillation at pH 4.5 following APHA 4500-CN-I [28]. A 100 mL aliquot was treated with 5 mL of 5% w/v lead acetate to precipitate interfering sulfides, which were removed by filtration through Whatman No. 4 paper. The clarified filtrate was transferred to a 500 mL boiling flask, and the pH was adjusted to 4.5 ± 0.1 with 0.5 M acetic acid. The sample was distilled under gentle boiling, and evolved HCN was trapped in a 50 mL receiver containing 0.25 M NaOH, then quantified by the pyridine-barbituric acid procedure described for CN_{Free} above.

Strong acid dissociable cyanide (CN_{SAD}) was determined by the operationally defined by-difference approach: $CN_{SAD} = CN_T - CN_{WAD}$. This is consistent with ASTM D4374 [30] as well as Parinyachet & Leepowpanth [31] and Tran et al. [32]. This standard procedure avoids non-standard sample manipulations while fully capturing cyanide complexes of iron, cobalt, gold, and platinum that require strongly acidic conditions for dissociation. Concentrations were calculated from individually determined CN_T and CN_{WAD} values.

Total cyanide (CN_T) was determined by acid reflux distillation following EPA SW-846 Method 9010C [29] and APHA 4500-CN—C [28]. A 100 mL aliquot was treated with 5 mL of 5% w/v zinc acetate to remove sulfides, then acidified to pH< 1 with 50 mL of 18 N sulfuric acid. Twenty millilitres of 2.5 M magnesium chloride ($MgCl_2$) were added as a catalytic agent to facilitate dissociation of thermodynamically stable iron- and cobalt-cyanide octahedral complexes. The mixture was refluxed at boiling under continuous airflow (290–350 mL min^{-1}) for one hour, with liberated HCN purged into a 50 mL gas scrubber containing 0.25 M NaOH. After cooling, the scrubber solution was transferred quantitatively to a 250 mL volumetric flask, diluted to volume, and quantified by the pyridine-barbituric acid colorimetric procedure at 578 nm using matrix-matched NaOH calibration standards over 0.01–2.50 mg CN^- L^{-1}.

Quality assurance, method validation, and analytical performance

Quality assurance and validation procedures were implemented to ensure analytical reliability. The workflow for interference control and matrix verification is outlined in Fig. 2. Key performance parameters, including detection limits, recovery, and precision, are summarized in Tables 1 and 2. The pyridine–barbituric acid spectrophotometric method demonstrated excellent linearity ($R^2 >$ 0.995), confirming its robustness for accurate determination of free and total cyanide in environmental samples.

The measured cyanide concentrations were benchmarked against national and international standards to evaluate human and ecological risk. Reference values included the Uganda National Environment Management Authority (NEMA) effluent limit (0.10 mg L^{-1}), the WHO drinking-water guideline (0.3–0.5 mg L^{-1}), the US EPA drinking-water Maximum Contaminant Level (MCL) (0.20 mg L^{-1}), aquatic criteria (acute ≈22 μg L^{-1}; chronic ≈5.2 μg L^{-1}) [14,36,37]. For solids, where no Ugandan guideline exists, results were

Table 4
Physicochemical characteristics and concentration (mg/L) of cyanide species for wastewater samples from plastic pipes, trenches, and metallic pipes around the tailing dump in the dry and wet seasons.

Sample	Temp (°C)	pH	Eh (mV)	EC (µS/cm)	CN_{Free}	CN_{WAD}	CN_{SAD}	CN_T
Plastic pipe wastewater — Dry season, n = 6								
PP-D1	22.40	5.12	526.8	7400	3.04	5.19	3.39	8.58
PP-D2	22.20	5.02	530.2	5300	0.98	8.08	9.58	17.66
PP-D3	23.10	4.98	541.4	6800	2.41	6.72	4.36	11.08
PP-D4	22.80	5.21	518.7	7100	3.52	5.84	4.10	9.94
PP-D5	23.40	4.87	558.3	8200	4.17	7.31	6.30	13.61
PP-D6	22.60	5.08	534.1	6600	2.88	6.14	4.10	10.24
Mean ± SD	22.75 ± 0.45	5.05 ± 0.12	535 ± 14	6900 ± 963	2.83 ± 1.09	6.55 ± 1.05	5.30 ± 2.31	11.85 ± 3.30
Plastic pipe wastewater — Wet season, n = 6								
PP-W1	24.10	5.38	482.1	4200	1.62	3.84	1.87	5.71
PP-W2	24.60	5.29	471.8	3800	0.74	5.12	5.08	10.20
PP-W3	25.20	5.44	465.3	4600	1.88	4.41	2.90	7.31
PP-W4	24.80	5.52	458.7	3500	1.24	3.29	1.67	4.96
PP-W5	25.60	5.31	474.9	5100	2.73	5.96	4.20	10.16
PP-W6	24.40	5.41	469.2	4100	1.54	4.18	2.42	6.60
Mean ± SD	24.78 ± 0.55	5.39 ± 0.09	470 ± 8	4217 ± 571	1.62 ± 0.67	4.47 ± 0.95	3.02 ± 1.35	7.49 ± 2.23
Trench wastewater — Dry season, n = 6								
TR-D1	18.80	7.82	367.9	3600	15.50	35.02	21.59	56.61
TR-D2	18.60	7.64	312.1	4200	7.04	7.52	10.20	17.72
TR-D3	19.20	7.74	341.5	3900	12.38	28.14	17.25	45.39
TR-D4	18.40	7.58	328.4	4050	8.62	9.87	12.36	22.23
TR-D5	19.50	7.91	358.2	3750	14.11	31.48	19.63	51.11
TR-D6	19.00	7.68	336.7	3820	10.44	18.72	14.75	33.47
Mean ± SD	18.92 ± 0.40	7.73 ± 0.12	341 ± 20	3887 ± 215	11.35 ± 3.25	21.79 ± 11.53	15.96 ± 4.35	37.76 ± 15.83
Trench wastewater — Wet season, n = 6								
TR-W1	21.40	7.51	331.4	2800	9.82	22.17	13.76	35.93
TR-W2	21.80	7.38	295.8	3100	4.51	5.38	6.56	11.94
TR-W3	22.10	7.44	314.7	2950	7.64	18.62	10.75	29.37
TR-W4	21.60	7.29	281.3	3300	5.28	6.74	7.75	14.49
TR-W5	22.40	7.55	322.9	2700	8.93	25.44	12.51	37.95
TR-W6	21.90	7.46	308.4	2870	6.82	14.38	9.66	24.04
Mean ± SD	21.87 ± 0.36	7.44 ± 0.09	309 ± 18	2953 ± 217	7.17 ± 2.05	15.46 ± 8.17	10.16 ± 2.75	25.62 ± 10.83
Metallic pipe wastewater — Dry season, n = 6								
MP-D1	21.80	3.24	784.7	10,400	7.09	7.79	7.57	15.36
MP-D2	22.30	3.11	801.4	11,200	8.42	8.91	9.03	17.94
MP-D3	21.50	3.38	762.8	9800	6.54	7.18	6.93	14.11
MP-D4	22.80	3.07	814.2	11,800	9.18	9.64	9.90	19.54
MP-D5	21.10	3.52	748.3	9200	5.87	6.52	6.18	12.70
MP-D6	21.60	3.31	778.4	10,600	7.64	8.24	8.18	16.42
Mean ± SD	21.85 ± 0.61	3.27 ± 0.17	782 ± 24	10,500 ± 936	7.46 ± 1.22	8.05 ± 1.14	7.96 ± 1.37	16.01 ± 2.50
Metallic pipe wastewater — Wet season, n = 6								
MP-W1	23.60	3.64	698.4	7800	4.82	5.34	5.10	10.44
MP-W2	24.10	3.58	712.1	8400	5.41	6.12	5.75	11.87
MP-W3	23.80	3.71	681.9	7200	4.14	4.87	4.36	9.23
MP-W4	24.40	3.49	724.8	8900	5.98	6.74	6.39	13.13
MP-W5	23.20	3.78	665.3	6800	3.67	4.28	3.86	8.14
MP-W6	23.90	3.62	706.2	8100	5.14	5.72	5.45	11.17
Mean ± SD	23.83 ± 0.41	3.64 ± 0.10	698 ± 22	7867 ± 774	4.86 ± 0.85	5.51 ± 0.88	5.15 ± 0.93	10.66 ± 1.80

compared with the Canadian soil quality criterion for free cyanide (0.9 mg kg^{-1}) [38].

Data analysis

Data handling and spatial mapping were performed in ArcGIS Pro 3.4 and Python 3.8. Concentration values below detection limits were substituted using MDL/2. Paired *t*-tests assessed seasonal differences, with effect sizes quantified by Cohen's d. Two-way ANOVA with Tukey HSD evaluated compartment and season effects, reporting partial eta-squared (η^2). Pearson correlation coefficient assessed relationships between cyanide fractions and physicochemical parameters ($p < 0.05$). Principal component analysis was done using singular value decomposition, generating biplots with group confidence ellipses across all matrices. Python libraries: pandas, numpy, scipy, statsmodels, scikit-learn, matplotlib, seaborn, and pingouin supported all computations.

Results and discussion

Seepage water at Busia Gold Fields was characterized by near-neutral pH (6.09–6.90), moderate EC (348–542 µS/cm), and CN_T ranging from 0.37 to 0.88 mg/L (dry) and 0.37–0.52 mg/L (wet) (Table 3). This represented a 49.5% seasonal reduction in CN_{Free}

Table 5
Physicochemical characteristics and concentration (mg/kg) of cyanide species in stream sediments during the dry and wet seasons.

Sample	Temp (°C)	pH	EC (μS/cm)	Eh (mV)	CN_{Free}	CN_{WAD}	CN_{SAD}	CN_T
Stratum 1 — Proximal zone (≤100 m) — Dry season, n = 7								
MD-P1	28.4	4.82	812	382	3.17	4.15	64.38	68.53
MD-P2	29.1	3.96	924	416	14.36	1.24	84.26	85.50
MD-P3	27.8	4.41	748	354	8.25	4.10	75.67	79.77
MD-P4	29.6	4.18	886	408	11.08	2.87	76.22	79.09
MD-P5	28.9	4.63	774	372	9.43	3.52	73.21	76.73
MD-P6	30.2	4.07	952	428	12.61	1.95	82.94	84.89
MD-P7	28.1	4.74	704	344	7.84	3.28	73.89	77.17
Mean ± SD	28.87 ± 0.85	4.40 ± 0.34	829 ± 94	386 ± 32	9.53 ± 3.66	3.02 ± 1.09	75.80 ± 6.63	78.81 ± 5.71
Stratum 1 — Proximal zone (≤100 m) — Wet season, n = 7								
MW-P1	24.2	5.18	672	336	2.50	3.74	59.31	63.05
MW-P2	24.8	4.38	762	368	12.23	1.11	77.55	78.66
MW-P3	23.9	4.84	618	308	7.06	3.69	69.70	73.39
MW-P4	25.1	4.62	734	358	9.04	2.58	70.18	72.76
MW-P5	24.6	5.04	642	324	7.65	3.17	67.42	70.59
MW-P6	25.4	4.51	788	378	10.09	1.75	76.35	78.10
MW-P7	23.7	5.12	584	298	6.53	2.95	68.05	71.00
Mean ± SD	24.53 ± 0.63	4.81 ± 0.32	686 ± 77	339 ± 31	7.87 ± 3.07	2.71 ± 0.98	69.79 ± 6.08	72.51 ± 5.25
Stratum 2 — Mid-gradient zone (100–500 m) — Dry season, n = 7								
MD-M1	27.6	5.84	524	286	4.13	3.62	64.06	67.68
MD-M2	28.3	6.42	382	214	6.60	5.98	53.04	59.02
MD-M3	27.1	6.12	448	248	5.47	4.83	57.64	62.47
MD-M4	28.8	5.68	562	304	3.89	5.21	59.52	64.73
MD-M5	27.4	6.28	406	228	4.74	4.46	53.66	58.12
MD-M6	29.2	5.74	538	292	7.12	3.94	64.50	68.44
MD-M7	27.9	6.38	374	218	5.28	5.63	55.37	61.00
Mean ± SD	28.04 ± 0.76	6.07 ± 0.31	462 ± 79	256 ± 38	5.32 ± 1.20	4.81 ± 0.87	58.26 ± 4.68	63.07 ± 4.05
Stratum 2 — Mid-gradient zone — Wet season, n = 7								
MW-M1	23.4	6.24	432	244	3.42	3.33	60.29	63.62
MW-M2	24.1	6.78	318	182	5.54	5.50	49.98	55.48
MW-M3	22.8	6.48	372	212	4.89	4.44	54.28	58.72
MW-M4	24.6	6.04	464	262	3.39	4.79	56.06	60.85
MW-M5	23.2	6.62	338	196	4.06	4.10	50.53	54.63
MW-M6	24.9	6.12	446	248	6.15	3.62	60.71	64.33
MW-M7	23.6	6.72	310	186	4.70	5.18	52.16	57.34
Mean ± SD	23.80 ± 0.76	6.43 ± 0.30	383 ± 64	219 ± 33	4.59 ± 1.04	4.42 ± 0.80	54.86 ± 4.38	59.28 ± 3.81
Stratum 3 — Distal/reference zone (>500 m) — Dry season, n = 6								
MD-D1	26.8	6.82	218	148	0.84	1.12	19.31	20.43
MD-D2	27.4	7.14	164	112	0.61	0.93	15.83	16.76
MD-D3	26.2	6.94	242	164	1.03	1.38	22.12	23.50
MD-D4	27.8	7.08	188	128	0.78	1.05	18.41	19.46
MD-D5	26.4	6.74	148	104	0.52	0.88	14.57	15.45
MD-D6	27.1	7.22	228	156	0.95	1.21	20.79	22.00
Mean ± SD	26.95 ± 0.61	6.99 ± 0.19	198 ± 37	135 ± 24	0.79 ± 0.20	1.09 ± 0.18	18.50 ± 2.88	19.60 ± 3.06
Stratum 3 — Distal/reference zone — Wet season, n = 6								
MW-D1	22.4	7.04	188	124	0.77	1.06	18.55	19.61
MW-D2	23.1	7.32	142	92	0.56	0.88	15.21	16.09
MW-D3	21.8	7.12	208	138	0.95	1.31	21.25	22.56
MW-D4	23.4	7.24	162	108	0.72	1.00	17.68	18.68
MW-D5	22.1	6.92	128	86	0.48	0.84	13.99	14.83
MW-D6	22.8	7.38	196	132	0.87	1.15	19.97	21.12
Mean ± SD	22.60 ± 0.61	7.17 ± 0.18	171 ± 32	113 ± 21	0.72 ± 0.18	1.04 ± 0.17	17.77 ± 2.77	18.82 ± 2.94

(paired *t*-test, $t = 11.314$, $p < 0.001$, $d = 4.619$). Surface water exhibited wider physicochemical variability (pH 4.24–6.64; EC up to 920 μS/cm) reflecting progressive downstream AMD influence, with CN_T of 0.16–0.42 mg/L (dry) declining by 47.4% in the wet season ($p = 0.015$). The CN_{SAD} fraction ranged from 0.05 to 0.50 mg/L across both compartments, consistent with free cyanide concentrations reported in ASGM-impacted surface and groundwater in Burkina Faso (0.009–2.42 mg/L), where seepage and surface runoff were identified as primary cyanide transport vectors from processing sites to receiving water bodies [15]. High levels of CN_{Free} have also been documented in dam and borehole water proximal to gold mining operations in the Brong-Ahafo Region of Ghana (21.70–25.09 mg/L), affirming that shallow seepage and surface runoff constitute recurrent and spatially consistent cyanide contamination pathways in sub-Saharan African ASGM settings [39].

Cyanide in seepage and surface water

Two-way ANOVA identified compartment identity as the dominant variance source for all CN fractions ($\eta^2 = 0.57$–0.66, $p < 0.001$), with a significant compartment × season interaction ($p < 0.001$–0.002) confirming greater seasonal dilution in seepage water than in

Table 6
Physicochemical characteristics and concentration (mg/kg) of cyanide species in tailings dumps during the dry and wet seasons.

Sample	Temp (°C)	pH	EC (μS/cm)	Eh (mV)	CN_{Free}	CN_{WAD}	CN_{SAD}	CN_T
Stratum A — Conventional tailings, active dumps — Dry season, n = 5								
AD-CA1	31.2	8.42	2248	284	5.90	1.75	33.04	34.79
AD-CA2	32.4	7.84	1864	318	4.15	5.40	28.49	33.89
AD-CA3	30.8	8.78	2612	248	6.42	2.31	35.99	38.30
AD-CA4	31.8	8.24	2084	304	5.07	3.18	30.95	34.13
AD-CA5	32.1	8.56	2384	272	4.63	2.84	31.34	34.18
Mean ± SD	31.66 ± 0.65	8.37 ± 0.36	2238 ± 285	285 ± 27	5.23 ± 0.92	3.10 ± 1.40	31.96 ± 2.78	35.06 ± 1.84
Stratum A — Conventional tailings, active dumps — Wet season, n = 5								
AW-CA1	26.8	8.18	1924	258	5.19	1.65	31.40	33.05
AW-CA2	27.6	7.62	1612	292	3.65	5.07	27.13	32.20
AW-CA3	26.4	8.54	2248	224	5.65	2.17	34.22	36.39
AW-CA4	27.2	8.02	1796	278	4.46	2.99	29.43	32.42
AW-CA5	27.4	8.32	2048	248	4.07	2.67	29.80	32.47
Mean ± SD	27.08 ± 0.48	8.14 ± 0.35	1926 ± 242	260 ± 26	4.60 ± 0.81	2.91 ± 1.31	30.40 ± 2.63	33.31 ± 1.75
Stratum B — Conventional tailings, abandoned dumps — Dry season, n = 5								
AD-CB1	29.4	6.24	748	184	0.91	1.75	5.53	7.28
AD-CB2	30.2	7.12	912	148	1.24	2.03	9.07	11.10
AD-CB3	28.8	6.58	624	212	0.78	1.62	6.25	7.87
AD-CB4	30.6	6.94	848	164	1.05	1.88	7.97	9.85
AD-CB5	29.1	5.96	564	228	0.63	1.49	4.81	6.30
Mean ± SD	29.62 ± 0.76	6.57 ± 0.48	739 ± 146	187 ± 33	0.92 ± 0.24	1.75 ± 0.21	6.73 ± 1.76	8.48 ± 1.96
Stratum B — Conventional tailings, abandoned dumps — Wet season, n = 5								
AW-CB1	25.2	6.48	624	158	0.89	1.72	5.41	7.13
AW-CB2	25.8	7.34	764	124	1.21	1.99	8.89	10.88
AW-CB3	24.6	6.82	524	184	0.76	1.59	6.12	7.71
AW-CB4	26.1	7.18	712	138	1.02	1.84	7.81	9.65
AW-CB5	24.9	6.22	472	198	0.61	1.46	4.71	6.17
Mean ± SD	25.32 ± 0.62	6.81 ± 0.47	619 ± 123	160 ± 31	0.90 ± 0.23	1.72 ± 0.21	6.59 ± 1.73	8.31 ± 1.92
Stratum C — Sand tailings, active dumps — Dry season, n = 5								
AD-SA1	33.8	9.24	2984	348	2.54	5.22	71.17	76.39
AD-SA2	34.6	8.86	2648	384	3.52	3.81	75.14	78.95
AD-SA3	33.2	9.68	3284	312	2.87	4.63	72.32	76.95
AD-SA4	34.1	9.12	2812	364	3.14	5.07	74.02	79.09
AD-SA5	33.5	9.44	3124	332	2.68	4.44	69.97	74.41
Mean ± SD	33.84 ± 0.54	9.27 ± 0.31	2970 ± 251	348 ± 28	2.95 ± 0.39	4.63 ± 0.56	72.52 ± 2.09	77.16 ± 1.94
Stratum C — Sand tailings, active dumps — Wet season, n = 5								
AW-SA1	28.4	8.96	2548	314	2.29	4.96	69.14	74.10
AW-SA2	29.2	8.62	2284	348	3.17	3.62	72.96	76.58
AW-SA3	27.8	9.42	2824	282	2.58	4.40	70.24	74.64
AW-SA4	28.8	8.84	2412	328	2.83	4.82	71.90	76.72
AW-SA5	28.1	9.18	2688	298	2.41	4.22	67.96	72.18
Mean ± SD	28.46 ± 0.55	9.00 ± 0.31	2551 ± 214	314 ± 26	2.66 ± 0.35	4.40 ± 0.53	70.44 ± 2.02	74.84 ± 1.89
Stratum D — Sand tailings, abandoned dumps — Dry season, n = 5								
AD-SB1	30.4	6.84	624	124	1.03	2.17	49.37	51.54
AD-SB2	31.2	7.42	512	88	0.74	1.89	44.81	46.70
AD-SB3	29.8	6.52	712	148	1.18	2.43	52.80	55.23
AD-SB4	31.6	7.18	548	104	0.88	2.05	47.79	49.84
AD-SB5	30.1	6.28	448	72	0.61	1.74	42.79	44.53
Mean ± SD	30.62 ± 0.76	6.85 ± 0.47	569 ± 102	107 ± 30	0.89 ± 0.23	2.06 ± 0.26	47.51 ± 3.91	49.57 ± 4.17
Stratum D — Sand tailings, abandoned dumps — Wet season, n = 5								
AW-SB1	25.8	7.04	524	104	1.02	2.15	48.88	51.03
AW-SB2	26.4	7.62	432	72	0.73	1.87	44.36	46.23
AW-SB3	25.2	6.72	608	124	1.17	2.41	52.27	54.68
AW-SB4	26.8	7.38	464	88	0.87	2.03	47.31	49.34
AW-SB5	25.5	6.48	378	56	0.60	1.72	42.37	44.09
Mean ± SD	25.94 ± 0.65	7.05 ± 0.47	481 ± 88	89 ± 27	0.88 ± 0.23	2.04 ± 0.26	47.04 ± 3.87	49.07 ± 4.13

surface water. In seepage, a unified hydrological control was evident from the near-perfect EC–CN_T relationship ($\rho = 0.972$, $p < 0.001$, $R^2 = 0.972$). In contrast, in surface water, CN_{Free} was decoupled from pH ($\rho = -0.116$, $p = 0.720$), yet CN_{WAD} remained positively correlated with EC ($\rho = 0.939$, $p < 0.001$). This indicates ongoing desorption of weakly complexed cyanide from contaminated bed sediments under AMD conditions rather than simple dilution. This persistence of CN_{WAD} during the wet season mirrors findings by [40] in ASGM-affected catchments in Burkina Faso, where cyanide transported via surface runoff and infiltration created diffuse catchment-wide contamination, with wet-season hydraulic redistribution delivering cyanide from processing zones to catchment outlets rather than achieving dilution-driven attenuation. These contrasting speciation dynamics between seepage and surface water reinforce the case for separate monitoring frameworks for each pathway, as increasingly advocated in recent ASGM literature [32,41].

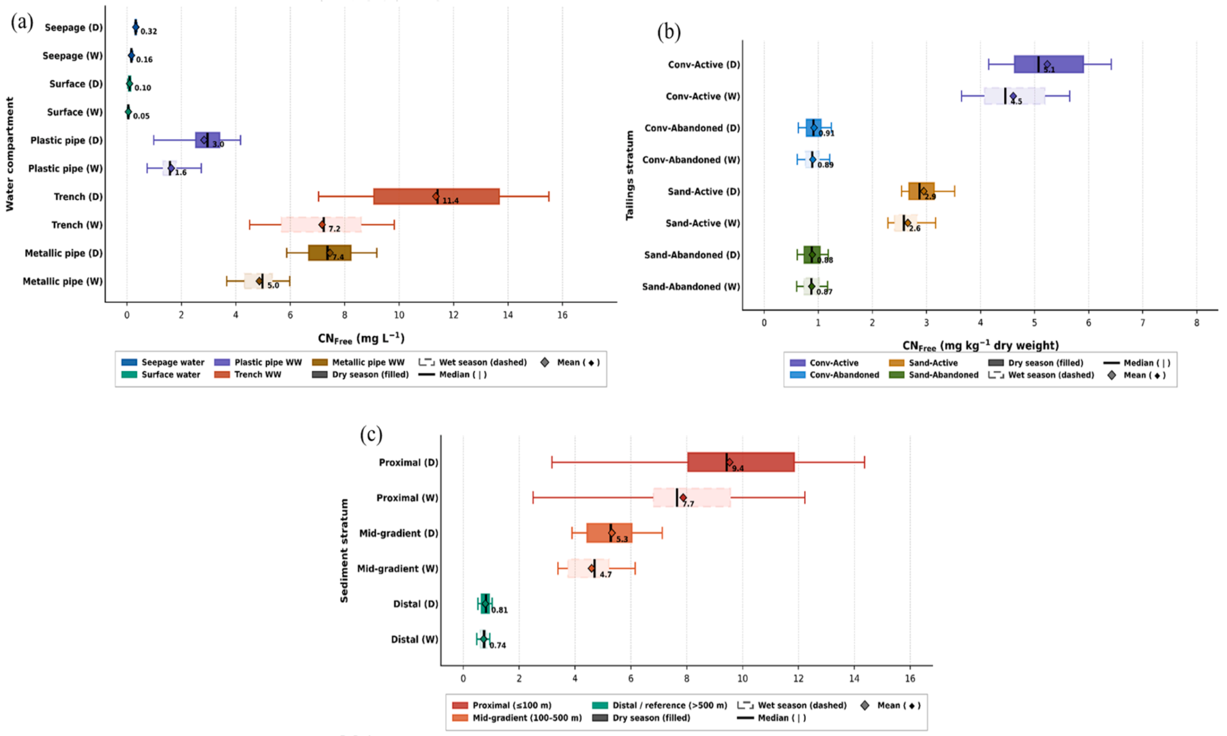

Fig. 3. Boxplots for the concentration of CN_{Free} in (a) water samples, (b) tailing dumps, and (c) stream sediments for the dry and wet seasons.

Cyanide in wastewater through plastic pipes, trenches, and metallic pipes

Wastewater discharged through trench, metallic pipe, and plastic pipe pathways recorded the highest cyanide concentrations across all sampled compartments, with distinct geochemical controls governing each pathway. Trench effluent (pH 7.29–7.91) yielded the greatest contamination, with CN_T peaking at 56.61 mg/L (dry season) and CN_{Free} declining by 36.8% in the wet season (paired *t*-test, $p < 0.001$), while redox potential emerged as the master variable (Eh vs CN_{Free}: $\rho = 0.986$, $p < 0.001$, $R^2 = 0.943$), consistent with [42] who demonstrated that under alkaline, oxidizing conditions, CN^- stability is governed primarily by Eh as oxidative conversion to CNO^- is kinetically suppressed at high redox and alkaline pH. Metallic pipe drainage exhibited the most extreme conditions — pH 3.07–3.78, EC up to 11,800 µS/cm, Eh reaching 814 mV as shown in Table 4, with a near-perfect negative pH–CN_{Free} relationship ($\rho = -0.993$, $p < 0.001$, $R^2 = 0.973$) attributable to acid-driven dissociation of metal-cyanide complexes from corroded infrastructure, as documented by [43]. Plastic pipe wastewater occupied an intermediate geochemical position (pH 4.87–5.52; CN_T 4.96–17.66 mg/L), with the highest within-group CN_{WAD} variability across all water compartments (3.29–8.08 mg/L), reflecting heterogeneous contributions from alkaline processing solutions and acid-weathered tailings leachate, consistent with speciation variability documented in ASGM wastewater attributed to site mining intensity, repeated cyanidation cycles, and proximity to active processing zones [15,40]. Two-way ANOVA confirmed that compartment identity dominated variance in pH ($\eta^2 = 0.986$) and Eh ($\eta^2 = 0.957$), indicating that the contrasting geochemical regimes are structurally determined by infrastructure type and processing chemistry rather than seasonal hydrological variation, with direct implications for source-specific cyanide management in ASGM settings [32,41].

Cyanide in stream sediments

Stream sediments at Busia Gold Fields exhibited a pronounced spatial contamination gradient across the three strata, with CN_{SAD}, the dominant fraction (85–93% of CN_T), declining from 59.31 to 84.26 mg/kg at proximal sites to 13.99–22.12 mg/kg at distal reference sites (Table 5). The inverse pH–CN_{SAD} relationship ($\rho = -0.954$, $p < 0.001$, $R^2 = 0.809$; slope $= -19.30$ mg/kg per pH unit) confirms that AMD-driven acidification at proximal sites promotes iron-cyanide complex accumulation in sediments, consistent with spatial CN enrichment gradients documented in ASGM-impacted sediments in Burkina Faso and Côte d'Ivoire, where cyanide concentrations declined systematically with distance from active cyanidation zones [23,44]. Significant seasonal reductions in CN_{Free} (17.4%, $p < 0.001$) were observed, though stratum identity dominated total variance ($\eta^2 = 0.954$ for CN_{SAD}, two-way ANOVA), indicating that spatial positioning relative to mining activity governs sediment cyanide burden more decisively than seasonal hydrological variation, consistent with spatial cyanide distributions in Burkina Faso ASGM catchments where proximity to active cyanidation zones consistently determined contamination intensity regardless of season [15].

Table 7
Pearson correlation coefficients (ρ) and significance levels (p-values) among cyanide species and physicochemical parameters in water samples, stream sediments, and tailing dumps.

Seepage water (n = 12)					Surface water (n = 12)			
Predictor	CN_{Free}	CN_{WAD}	CN_{SAD}	CN_T	CN_{Free}	CN_{WAD}	CN_{SAD}	CN_T
pH	**0.972*****	**0.951*****	**0.975*****	**0.972*****	−0.116 ns	**−0.778****	−0.386 ns	−0.646*
	< 0.001	< 0.001	< 0.001	< 0.001	0.717	0.003	0.215	0.024
Temperature (°C)	**−0.797****	**−0.811****	**−0.800****	**−0.797****	−0.351 ns	−0.161 ns	−0.060 ns	−0.109 ns
	0.002	0.001	0.002	0.002	0.264	0.615	0.852	0.736
EC (µS/cm)	**0.972*****	**0.986*****	**0.958*****	**0.972*****	0.362 ns	**0.939*****	0.554 ns	**0.853*****
	< 0.001	< 0.001	< 0.001	< 0.001	0.248	0.001	0.062	< 0.001
Eh (mV)	**0.958*****	**0.951*****	**0.954*****	**0.958*****	0.151 ns	0.807**	0.418 ns	0.689*
	< 0.001	< 0.001	< 0.001	< 0.001	0.638	0.002	0.178	0.013
Plastic pipe wastewater (n = 12)					Trench wastewater (n = 12)			
pH	−0.455 ns	**−0.902*****	**−0.799****	**−0.888*****	**0.874*****	0.755**	**0.874*****	0.755**
	0.137	< 0.001	0.002	< 0.001	< 0.001	0.005	< 0.001	0.005
Temperature (°C)	−0.273 ns	−0.552 ns	−0.354 ns	−0.490 ns	−0.385 ns	−0.084 ns	−0.385 ns	−0.084 ns
	0.390	0.063	0.259	0.106	0.216	0.796	0.216	0.796
EC (µS/cm)	**0.846*****	0.720**	0.476 ns	0.573 ns	0.203 ns	−0.077 ns	0.203 ns	−0.077 ns
	< 0.001	0.008	0.118	0.051	0.527	0.812	0.527	0.812
Eh (mV)	0.559 ns	**0.839*****	0.648*	0.783**	**0.986*****	**0.895*****	**0.986*****	**0.895*****
	0.059	< 0.001	0.023	0.003	< 0.001	< 0.001	< 0.001	< 0.001
Metallic pipe wastewater (n = 12)					Stream sediments, all strata (n = 40)			
pH	**−0.993*****	**−0.993*****	**−0.993*****	**−0.993*****	**−0.859*****	−0.312*	**−0.954*****	**−0.955*****
	< 0.001	< 0.001	< 0.001	< 0.001	< 0.001	0.049	< 0.001	< 0.001
Temperature (°C)	−0.448 ns	−0.448 ns	−0.448 ns	−0.448 ns	0.477**	0.240 ns	0.488**	**0.514*****
	0.143	0.143	0.143	0.143	0.002	0.136	0.001	< 0.001
EC (µS/cm)	**0.993*****	**0.993*****	**0.993*****	**0.993*****	**0.864*****	0.372*	**0.970*****	**0.972*****
	< 0.001	< 0.001	< 0.001	< 0.001	< 0.001	0.018	< 0.001	< 0.001
Eh (mV)	**0.986*****	**0.986*****	**0.986*****	**0.986*****	**0.860*****	0.371*	**0.969*****	**0.970*****
	< 0.001	< 0.001	< 0.001	< 0.001	< 0.001	0.018	< 0.001	< 0.001
Tailings dumps, all strata (n = 40)								
pH	**0.701*****	**0.766*****	**0.658*****	**0.660*****				
	< 0.001	< 0.001	< 0.001	< 0.001				
Temperature (°C)	0.381*	0.499**	0.416**	0.439**				
	0.015	0.001	0.007	0.005				
EC (µS/cm)	**0.778*****	**0.733*****	0.482**	0.486**				
	< 0.001	< 0.001	0.002	0.002				
Eh (mV)	**0.690*****	**0.680*****	0.361*	0.367*				
	< 0.001	< 0.001	0.022	0.020				

Cell Contents: Pearson correlation coefficient (ρ) P-Value.
* Significant correlation at the 0.05 level.
** Significant correlation at the 0.01 level.
*** Significant correlation at the 0.001 level.

Cyanide in tailing dumps

Tailings dumps at Busia Gold Fields exhibited the widest range of cyanide concentrations across all solid matrices, with CN_{SAD} and CN_T values reflecting strong differentiation by both stratum type and operational status (Table 6). Sand-active tailings recorded the highest CN_T (72.18–79.09 mg/kg) and CN_{SAD} (67.96–75.14 mg/kg) across both seasons, attributable to sustained alkaline cyanidation inputs (pH 8.62–9.68) maintaining CN^- stability. However, conventional-abandoned tailings yielded the lowest concentrations (CN_T 6.17–11.10 mg/kg) following progressive weathering and attenuation of residual cyanide, a status-dependent attenuation pattern consistent with [45], who documented accelerated CN_T depletion in abandoned ASGM tailings under ambient oxidation. Two-way ANOVA confirmed that tailings type dominated variance in CN_{SAD} ($\eta^2 = 0.716$–0.736) while operational status governed CN_{Free} ($\eta^2 = 0.744$) and pH ($\eta^2 = 0.820$), reflecting the contrasting roles of processing chemistry intensity and abandonment-induced weathering. Seasonal reductions in CN_{Free} were significant across active strata (10.0–12.0%, $p < 0.001$) but negligible in abandoned strata, where dry and wet season values were virtually identical, confirming complete temporal stabilization of labile cyanide in fully weathered tailings. This confirms complete temporal stabilization of labile cyanide in fully weathered tailings, consistent with [46], who demonstrated that CN_{WAD} and CN_T were undetectable in aged gold mine tailings (6–9 years), with reactive cyanide species having been eliminated through progressive volatilization, leaching, and microbial degradation. The positive pH–CN_{Free} relationship ($\rho = 0.701$, $p < 0.001$), sign-reversed relative to sediments, reflects alkaline stabilization of free cyanide unique to active processing environments, while EC–CN_{Free} ($\rho = 0.778$, $p < 0.001$) confirmed that ionic load, as a proxy for reagent application intensity, was a reliable predictor of labile cyanide retention across all tailing's strata and seasons [32].

Box plots of CN_{Free} across all sampling matrices as shown in Fig. 3 revealed clear concentration hierarchies and consistent seasonal patterns. In water samples, trench wastewater recorded the highest median CN_{Free} (11.4 mg/L dry; 7.2 mg/L wet) and the widest interquartile range, reflecting redox-driven variability, while seepage and surface water remained near zero across both seasons.

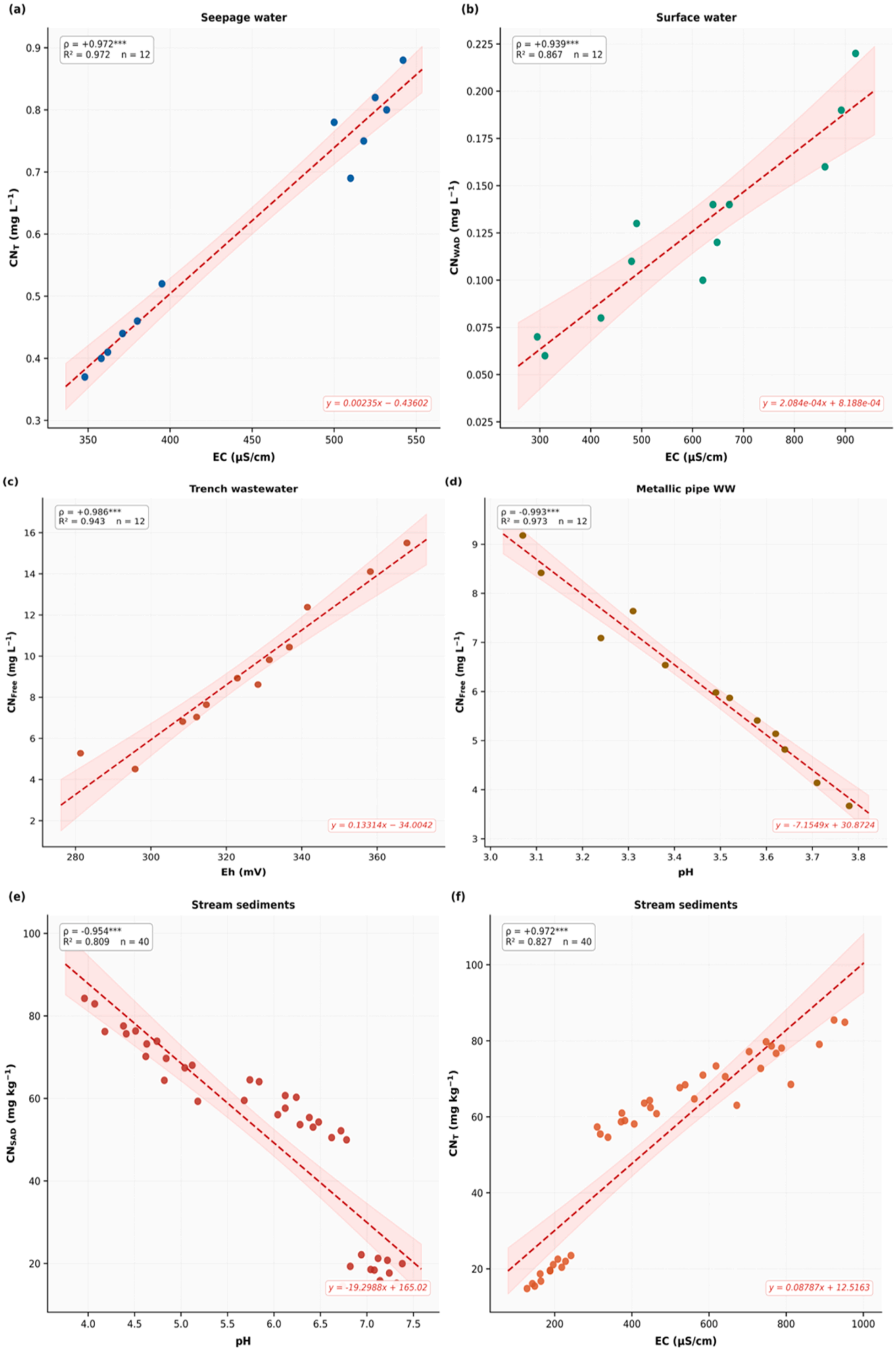

Fig. 4. Scatter plots with ordinary least-squares regression lines (dashed red) and 95% confidence intervals (shaded band) illustrating selected mechanistic relationships between physicochemical parameters and cyanide fractions across all sampling matrices: (a) seepage water (b) surface water (c) trench wastewater (d) metallic pipe wastewater (e) stream sediments (f) stream sediments (g) tailings dumps, and (h) tailings dumps. ρ = Spearman rank-correlation coefficient; R^2 = coefficient of determination.

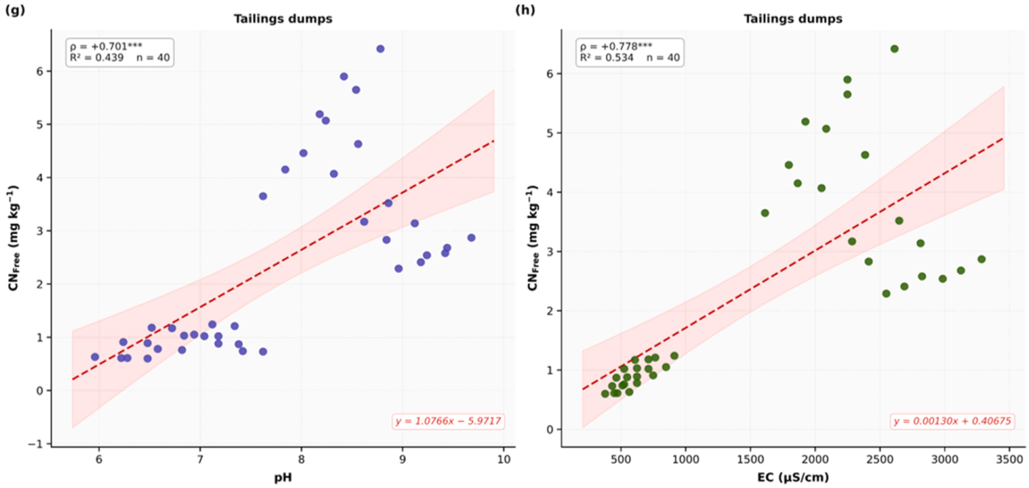

Fig. 4. (*continued*).

Stream sediment CN_{Free} decreased systematically from proximal (9.4 mg/kg dry) to distal strata (0.81 mg/kg dry), confirming the spatial AMD contamination gradient. Among tailings, conventional-active dumps yielded the highest CN_{Free} medians (5.1 mg/kg dry), with sand-abandoned and conventional-abandoned strata showing negligible seasonal shifts, indicating complete temporal stabilization of labile cyanide in weathered materials.

Pearson correlation analysis revealed matrix-specific geochemical controls on CN_{Free} across all sampling compartments (Table 7). In seepage water, all physicochemical parameters correlated strongly with CN_{Free} ($\rho = 0.95$–0.99, $p < 0.001$), confirming unified hydrological control, whereas surface water CN_{Free} was decoupled from pH ($\rho = -0.116$, $p = 0.720$) despite CN_{WAD} remaining significantly correlated with EC ($\rho = 0.939$, $p < 0.001$). Trench wastewater was dominated by Eh ($\rho = 0.986$, $p < 0.001$), while metallic pipe drainage exhibited near-perfect correlations across all variables ($\rho = \pm 0.993$, $p < 0.001$). In stream sediments, pH showed the strongest inverse relationship with CN_{SAD} ($\rho = -0.954$, $p < 0.001$), whereas EC was positively correlated with CN_T ($\rho = 0.972$, $p < 0.001$), collectively encoding the AMD spatial gradient. In tailings, the pH–CN_{Free} relationship was positive ($\rho = 0.701$, $p < 0.001$), sign-reversed relative to sediments, reflecting alkaline stabilization.

The eight selected scatter plots quantified the dominant mechanistic relationships between physicochemical parameters and cyanide fractions across all matrices (Fig. 4). EC explained 97.2% of CN_T variance in seepage water ($\rho = 0.972$, $R^2 = 0.972$), confirming hydrological dilution control, while Eh emerged as the master variable in trench wastewater ($\rho = 0.986$, $R^2 = 0.943$), consistent with [42]. The near-perfect negative pH–CN_{Free} relationship in metallic pipe drainage ($\rho = -0.993$, $R^2 = 0.973$) confirmed acid-driven complex dissociation [43], while the sign reversal between sediment pH–CN_{SAD} ($\rho = -0.954$) and tailings pH–CN_{Free} ($\rho = 0.701$) captured the mechanistic contrast between AMD-driven accumulation and alkaline processing stabilization, a geochemical duality increasingly documented in ASGM environments [32]. Regression equations further quantified that every unit pH decline in proximal sediments corresponded to 19.30 mg/kg additional CN_{SAD} accumulation, and every 1 μS/cm EC increase in tailings predicted 0.0013 mg/kg additional CN_{Free} retention.

PCA biplots explained 76.9% (solids) and 92.0% (water) of total variance across PC1 and PC2, providing robust multivariate separation of all sampling groups (Fig. 5). In the solids biplot, PC1 encoded the contamination gradient, CN_{SAD}, CN_T, and Eh loading strongly leftward toward contaminated proximal sediments and sand-active tailings, while PC2 separated sediment and tailings matrices along the pH axis, reflecting the opposing AMD acidification and alkaline cyanidation signatures, consistent with multivariate geochemical cluster analyses in ASGM-impacted environments that distinguished anthropogenic contamination signatures from geogenic backgrounds [47]. In the water biplot, the near-perpendicular orientation of pH and Eh loading vectors visually confirmed the geochemical dichotomy between alkaline redox-controlled trench effluent and severely acidic metallic pipe drainage, while all four CN fraction vectors aligned co-linearly along PC1, corroborating their shared hydrological and processing controls [32]. Confidence ellipses demonstrated complete between-group separation for all seven solid matrix clusters and all five water compartments across both seasons.

Cyanide concentrations across sampled matrices generally exceeded national and international thresholds, although not uniformly. All 60 water samples surpassed the Uganda NEMA standard ($CN_T > 0.10$ mg/L). WHO/FAO irrigation guideline (0.05 mg/L). At the same time, 55 of 60 exceeded the US EPA MCL (0.20 mg/L) and 43 of 60 the WHO short-term guideline (0.50 mg/L), indicating that 17 samples, predominantly wet-season seepage and surface water, remained below the short-term threshold following seasonal dilution. Trench wastewater exceeded the US EPA chronic aquatic life criterion (0.0052 mg/L) by up to 2981-fold, consistent with extreme ASGM contamination documented by Marshall et al. [48] and Freitas & Horta [10]. For solid matrices, all 80 samples exceeded the CCME guideline (0.9 mg/kg), while 8 of 40 tailings samples, exclusively conventional-abandoned and sand-abandoned strata, remained below the ICMC tailings storage target [49], reflecting post-abandonment cyanide attenuation consistent with Welman-purchase et al. [50] and Bowell [51].

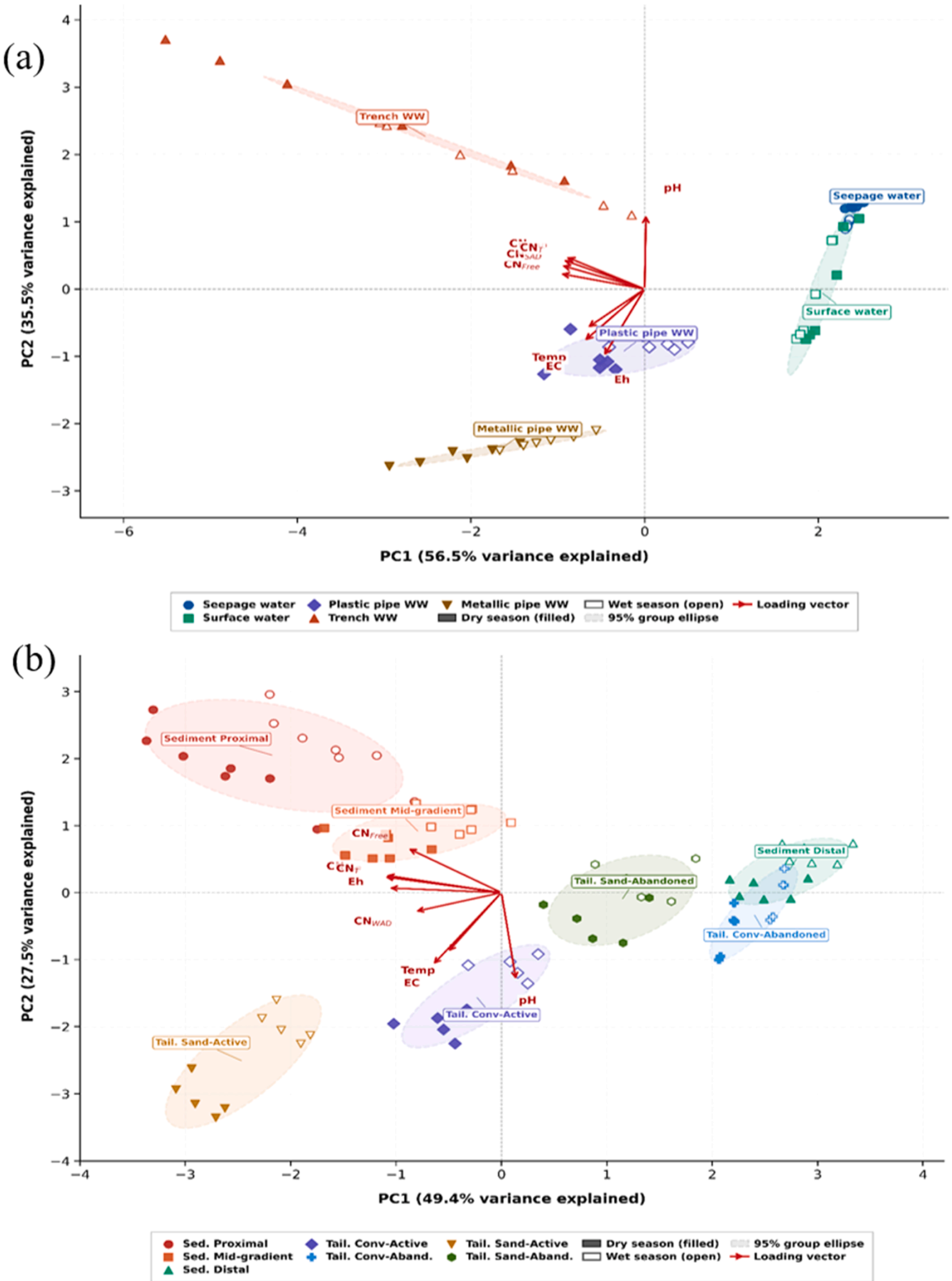

Fig. 5. Principal component analysis (PCA) biplot of physicochemical parameters and cyanide speciation fractions for; (a) water samples across five compartments with PC1 and PC2 accounting for 56.5% and 35.5% of total variance, respectively (cumulative 92.0%) and (b) stream sediments and tailings dump samples with PC1 and PC2 accounting for 49.4% and 27.5% of total variance, respectively (cumulative 76.9%).

Policy and management implications

Cyanide concentrations across all water and solid matrices at Busia Gold Fields exceeded Uganda's NEMA effluent limit (Table 8). Trench wastewater exceeded limits by up to 566-fold, while wet-season seepage remained contaminated across all sampled points. All 80 sediment and tailings samples exceeded CCME solid-matrix guidelines, confirming widespread contamination across solid environmental compartments. Effective management requires a two-pronged strategy: (1) regulatory strengthening through routine monitoring benchmarked against WHO, US EPA, and ICMC thresholds, clear chemical-use permitting, and integration with Uganda's Mining and Minerals Act and ASGM National Action Plan; and (2) source-specific mitigation targeting high-risk discharge points, particularly trench and metallic pipe outlets, where CN_{Free} exceeded the US EPA chronic aquatic life criterion by up to 2981-fold,

Table 8
Comparison of measured cyanide concentrations with selected national and international benchmarks (values, exceedance factors, and number of analytical units exceeding each benchmark).

No.	Matrix / metric	Measured summary	Benchmark (source)	Benchmark value	Analytical units exceeding	Max/ benchmark (≈)
Water samples — CN_T and CN_{Free} (n = 60 per season per parameter; 5 compartments × 2 seasons × 6 sites)						
1	Water — all compartments (CN_T)	Range 0.12–56.61 mg L^{-1}; max 56.61 mg L^{-1} (TR-D1, trench dry); mean 11.11 mg L^{-1}; dry season max 56.61, wet season max 37.95 mg L^{-1}	Uganda NEMA — effluent limit (cyanide) [14]	0.10 mg L^{-1}	60/60 —all samples in all compartments and both seasons exceed this limit	56.61 / 0.10 ≈ 566 ×
2	Water — all compartments (CN_T)	Same as row 1	US EPA — drinking-water Maximum Contaminant Level (MCL) [52]	0.20 mg L^{-1}	55/60 —only 5 wet-season seepage and surface water samples fall below this threshold	56.61 / 0.20 ≈ 283 ×
3	Water — all compartments (CN_T)	Same as row 1	WHO — long-term health-based reference value for cyanide in drinking water [36]	0.30 mg L^{-1}	50 / 60	56.61 / 0.30 ≈ 189 ×
4	Water — all compartments (CN_T)	Same as row 1	WHO — short-term health-based value [36]	0.50 mg L^{-1}	43/60	56.61 / 0.50 ≈ 113 ×
5	Water — all compartments (CN_{Free}) Chronic aquatic criterion	CN_{Free} range 0.02–15.50 mg L^{-1}; min seepage (SW-W5) = 0.13 mg L^{-1}; max trench dry (TR-D1) = 15.50 mg L^{-1}; all compartments exceed chronic criterion in both seasons	US EPA — aquatic life criteria (freshwater), chronic [37]	5.2 μg L^{-1} (0.0052 mg L^{-1})	60/60 — all 60 samples exceed the chronic aquatic criterion; minimum ratio is SW-W5 (0.13 mg/L ÷ 0.0052) ≈ 25 × above chronic limit	15.50 / 0.0052 ≈ 2981 × (TR-D1 CN_{Free})
6	Water — all compartments (CN_{Free}) Acute aquatic criterion	Same CN_{Free} data as row 5	US EPA — aquatic life criteria (freshwater), acute [37]	22 μg L^{-1} (0.022 mg L^{-1})	59/60 — only one sample (SS-W4, CN_{Free} = 0.02 mg L^{-1}) falls marginally below the acute criterion	15.50 / 0.022 ≈ 705 ×
Stream sediment samples — CN_T (n = 40; 20 sites × 2 seasons; 3 spatial strata)						
7	Stream sediments (CN_T)	Range 14.83–85.50 mg kg^{-1} dry weight; max 85.50 mg kg^{-1} (MD2 dry season, proximal stratum); min 14.83 mg kg^{-1} (MD-D5 wet season, distal stratum); mean 53.65 mg kg^{-1} across all strata and seasons	CCME — Canadian soil quality guideline for free cyanide (residential/ agricultural land use) [38]	0.9 mg kg^{-1}	40/40 — all sediment samples in all strata and both seasons exceed this guideline; even the lowest distal wet-season value (14.83 mg kg^{-1}) exceeds the guideline by 16 ×	85.50 / 0.9 ≈ 95 ×
Tailings dump samples — CN_T (n = 40; 20 sites × 2 seasons; 4 strata: conventional/sand × active/abandoned)						
8	Tailings dumps (CN_T)	Range 6.17–79.09 mg kg^{-1}; max 79.09 mg kg^{-1} (AB-SA4 dry, sand active); min 6.17 mg kg^{-1} (AB-CB5 wet, conventional abandoned); mean 41.97 mg kg^{-1}; sand active mean 75.96 mg kg^{-1} vs conventional abandoned mean 7.90 mg kg^{-1}	CCME — Canadian soil quality guideline for free cyanide (residential/ agricultural land use) [38]	0@#@.9 mg kg^{-1}	40/40 — all tailings' samples in all strata and both seasons exceed this guideline; conventional abandoned dumps (lowest contamination) still exceed by 7–12 ×	79.09 / 0.9 ≈ 88 ×

through processing circuit containment, cyanide detoxification before discharge, and structural rehabilitation of sand-active tailings, which recorded the highest solid-phase CN_T (up to 79.09 mg/kg) across both seasons. Seasonal dilution demonstrably failed to achieve compliance in any compartment, reinforcing that operational intervention rather than natural attenuation must anchor the management response. This is consistent with recommendations from regional ASGM assessments and global cyanide-management literature [4,32].

Practical remediation and management options

Effective cyanide remediation at Busia Gold Fields requires integrated containment, destruction, polishing, and secure tailings management scaled to measured contamination profiles. Immediate source control through lined tailings ponds, flow equalization, and community advisories is essential [53], prioritizing trench and metallic pipe discharge points where CN_{Free} reached 15.50 mg/L and 9.18 mg/L, respectively. Alkaline chlorination suits seepage and surface water ($CN_{T<}$0.88 mg/L), while the INCO SO_2/air process is appropriate for larger trench wastewater volumes where CN_{WAD} peaked at 35.02 mg/L [54,55]. Advanced oxidation using ozone or Fenton reagents is warranted for metallic pipe drainage, given its refractory metal-cyanide complexes under severely acidic, high-EC conditions, while polishing with activated carbon and passive systems, biofilters, and constructed wetlands, provides cost-effective long-term treatment for dilute wet-season effluents where seasonal CN_{Free} reductions of 34.8–49.5% though operationally demanding [56,57]. Sand-active tailings (CN_T up to 79.09 mg/kg) and proximal sediments (CN_{SAD} up to 84.26 mg/kg) require solid-phase stabilization, engineered capping, or controlled reprocessing under monitored alkaline conditions to prevent further leachate migration into receiving stream sediments [58]. All treatment systems must incorporate alkaline pH control, oxidant quenching, and continuous multi-fraction cyanide monitoring, given the demonstrated inter-compartment speciation variability across both seasons.

Conclusion

Cyanide contamination at Busia Gold Fields is governed by matrix-specific hydrochemical gradients controlling speciation, mobility, and persistence. Elevated pH and EC promoted CN_{Free} and CN_{WAD} retention in effluents, while high Eh and ionic strength enhanced CN_{SAD} accumulation. CN_{SAD} reached 84.26 mg/kg in downstream sediments, while sand-active tailings recorded CN_T up to 79.09 mg/kg. The pH–CN_{Free} relationship reversed between sediments ($\rho = -0.954$) and tailings ($\rho = +0.701$), reflecting contrasting geochemical controls. This reversal captures the mechanistic duality between AMD-driven acidification and alkaline cyanidation stabilization processes. Dry-to-wet seasonal CN_{Free} reductions of 34.8–49.5% ($p < 0.001$) failed to achieve compliance across all 140 samples. Wet-season hydraulic flushing redistributes cyanide from contaminated solids into receiving waters, amplifying rather than reducing ecological risk. These findings demonstrate that seasonal dilution is an unreliable assumption for cyanide risk mitigation in ASGM environments. Universal exceedance of NEMA, WHO, US EPA, and CCME thresholds highlights the inadequacy of current regulatory oversight. Urgent interventions are required, including source-specific remediation at trench and metallic pipe discharge points. Structural rehabilitation of active tailings and effective sediment leachate containment measures are also necessary. This study establishes a comprehensive cyanide speciation baseline for Ugandan ASGM systems. It provides actionable evidence supporting the integration of multi-fraction monitoring into NEMA compliance frameworks and the Mining and Minerals Act. Future research should evaluate the bioremediation potential and quantify the influence of tailings age and disposal practices.

Ethics approval statement

This article does not contain any studies with human participants or animals performed by any of the authors.

CRediT authorship contribution statement

Denis Musiige: Conceptualization, Data curation, Writing – original draft. **Jhonnah Mundike:** Supervision, Methodology, Formal analysis, Writing – review & editing. **Cuthbert Makondo:** Supervision, Writing – review & editing.

Declaration of competing interest

The authors declare that they have no known competing financial interests or personal relationships that could have appeared to influence the work reported in this paper.

Funding statement

This work was supported by the Copperbelt University Africa Center of Excellence for Sustainable Mining (CBU ACESM), at The Copperbelt University, Kitwe, Zambia.

Supplementary materials

Supplementary material associated with this article can be found, in the online version, at doi:10.1016/j.sciaf.2026.e03514.

References

[1] D. Musiige, J. Mundike, C. Makondo, Evaluation of potentially toxic metals in tailings from Busia gold mine fields of eastern Uganda, J. Clean. Prod. 469 (2024), https://doi.org/10.1016/j.jclepro.2024.143222.
[2] B. Nagudi, Status of geological resources in uganda for the embassy of the Republic of Korea in Uganda, Kampala (2011).
[3] C. Nyakecho, S.G. Hagemann, An overview of gold systems in Uganda, Aust. J. Earth Sci. An Int. Geosci. J. Geol. Soc. Aust. 611 (2014) 37–41, https://doi.org/10.1080/08120099.2013.831773.
[4] UNEP, The national action plan for artisanal and small scale gold mining in uganda, in accordance with the minamata convention on mercury. https://www.nema.go.ug/sites/default/files/NAP%202019%20LATEST.pdf.
[5] M.A. Ondayo, M.J. Watts, C.J. Mitchell, D.C.P. King, O. Osano, Review: artisanal gold mining in Africa—environmental pollution and human health implications, Expo. Heal. (2023), https://doi.org/10.1007/s12403-023-00611-7.
[6] T. Omara, S. Karungi, S. Ssebulime, K.M. Kiplagat, O. Bongomin, R. Ogwang, Artisanal and small-scale gold mining in Syanyonja, Busia Gold District, South Eastern Uganda: impacts on the mining population and the environment, Asian J. Geol. Res. 2 (4) (2019) 1–13.
[7] S.A. Abdul-wahab, F.A. Marikar, The environmental impact of gold mines: pollution by heavy metals, Cent, Eur. J. Eng. 2 (2) (2012), https://doi.org/10.2478/s13531-011-0052-3.

[8] E. Fagbenro, A.A. Yinusa, T.S. Ajekiigbe, K.M. Oke, A.O. Obiajunwa, Assessment of heavy metal pollution in Osun State, Nigeria using proton-induced X-ray emission, Sci. African (2021), https://doi.org/10.1016/j.sciaf.2021.e01047.
[9] A.M.R. Leung, J.L.D.P. Lu, Environmental health and safety hazards of indigenous small-scale gold mining using cyanidation in the philippines, Environ. Health Insights 10 (2016) 125–131, https://doi.org/10.4137/EHI.S38459.
[10] J. Freitas, D. Horta, Impacts of cyanide in gold mining and cyanide removal methodologies in liquid waste from gold processing, Rev. Metal 59 (3) (2023), https://doi.org/10.3989/revmetalm.247.
[11] R. Eisler, S.N. Wiemeyer, Cyanide hazards to plants and animals from gold mining and related water issues, Rev. Environ. Contam. Toxicol. 183 (2004) 21–54, https://doi.org/10.1007/978-1-4419-9100-3_2.
[12] UNEP, Analysis of formalization approaches in the ASGM sector based on experiences in Ecuador, Mongolia, Peru, Tanzania and Uganda (2012). https://www.unep.org/globalmercurypartnership/resources/report/analysis-formalization-approaches-asgm-sector-based-experiences-ecuador-mongolia.
[13] The Republic of Uganda, Ministry of energy and mineral development, energy and mineral development sector, sector development plan 2015/16 – 2019/20, (2015). https://www.npa.go.ug/wp-content/uploads/2023/03/Energy-Sector-Development-plan-Final.pdf.
[14] NER (National Environmental Regulations), The national environment (Standards for Discharge of Effluent into Water or on Land) regulations. https://www.nemaug.org/regulations/effluent_discharge_regulations.pdfage, 1999.
[15] E.N. Kohio, S.K. Sossou, H. Karoui, H. Yacouba, Environmental cyanide pollution from artisanal gold mining in Burkina Faso: human exposure risk analysis based on a conceptual site model, Int. J. Environ. Res. Public Health. 22 (7) (2025), https://doi.org/10.3390/ijerph22071125.
[16] C. Anning, J. Wang, P. Chen, I. Batmunkh, X. Lyu, Determination and detoxification of cyanide in gold mine tailings: a review, Waste Manag. Res. 37 (11) (2019) 1117–1126, https://doi.org/10.1177/0734242X19876691.
[17] R.S. Ghosh, J.C.L. Meeussen, D.A. Dzombak, D.V Nakles, Fate and transport of anthropogenic cyanide in soil and groundwater, in cyanide in water and soil, Chem. Risk Manag. 11 (1) (2006) 191–207, https://doi.org/10.1201/9781420032079.ch10.
[18] A.S. Akingboye, A.A. Bery, A.C. Ogunyele, J. Gnapragasan, T. Adewumi, A.V. Oyeshomo, O.C. Akakuru, O. Balogun, Magneto-radiometric and geochemical mapping of structurally controlled hydrothermal gold mineralization in the Okpella Neoproterozoic terrain, Igarra Schist Belt, SW Nigeria, Sci. African (2025), https://doi.org/10.1016/j.sciaf.2025.e02960.
[19] A.S. Akingboye, A.A. Bery, A.C. Ogunyele, M.D. Dick, T.O. Ale, E.A. Titus, Magnetic-Assisted Radiometric, Speciation, and Environmental Studies of an Orogenic Gold Terrain: okpella, Igarra Schist Belt, SW Nigeria, Earth Syst. Environ. 9 (2025) 2277–2306, https://doi.org/10.1007/s41748-025-00704-0.
[20] S.O. Obaje, A.C. Ogunyele, A.O. Adeola, A.S. Akingboye, Assessment of stream sediments pollution by potentially toxic elements in the active mining area of Okpella, Edo State, Nigeria, Mining-Geology-Petroleum Eng. Bull. 34 (2) (2019) 43–49, https://doi.org/10.17794/rgn.2019.2.5.
[21] O.A.E. Abdalla, F.O. Suliman, H. Al-Ajmi, T. Al-Hosni, H. Rollinson, Cyanide from gold mining and its effect on groundwater in arid areas, Yanqul mine of Oman, Environ. Earth Sci. 60 (4) (2010) 885–892, https://doi.org/10.1007/s12665-009-0225-z.
[22] B.G. Lottermoser, Mine Wastes Characterization, Treatment, Environmental Impacts, 2nd edn, Springer Berlin Heidelberg, Cairns, Queensland, 2007, 4870.
[23] L.C. Razanamahandry, H.A. Andrianisa, H. Karoui, J. Podgorski, H. Yacouba, Prediction model for cyanide soil pollution in artisanal gold mining area by using logistic regression, Catena 1 (62) (2018) 40–50, https://doi.org/10.1016/j.catena.2017.11.018.
[24] A.B. Mbonimpa, E. Barifaijo, J.V Tiberindwa, The potential for gold mineralisation in the greenstone belt of Busia District, South Eastern Uganda, African J. Sci. Technol. Sci. Eng. Ser. 8 (1) (2007) 116–134.
[25] E. Sifuel Gomezulu, A. Mwakaje, H. Katima, Heavy metals and cyanide distribution in the villages surrounding Buzwagi Gold Mine in Tanzania, Tanzania J. Sci. 44 (1) (2018) 107–122. https://www.tjs.udsm.ac.tz.
[26] C. Mbare, M. Said, R. Minja, Determination of cyanide concentration levels in surface water and soil from artisanal small-scale gold mining villages at Chunya, Mbeya-Tanzania, Tanzania J. Eng. Technol. 42 (2) (2023) 55–64, https://doi.org/10.52339/tjet.v42i2.913.
[27] Uganda National Meteorological Authority (UNMA), The state of climate of Uganda 2021. https://www.unma.go.ug/download/state-of-climate-of-uganda-in-2021/?wpdmdl=1403&refresh=63abb8063b8c31672198150, 2022.
[28] American Public Health Association, APHA method 4500-CN-Cyanide, APHA method 4500-CN stand, Methods Exam. Water Wastewater 552 (1992) 18–35.
[29] E.P.A. US, SW-846 test method 9013A. cyanide extraction procedure for solids and Oils, United States Environ, Prot. Agency (2014) 1–13.
[30] ASTM, Standard test methods for cyanides in water–Automated methods for total cyanide, acid dissociable cyanide, and thiocyanate, 2000, pp. 10–11. https://standards.globalspec.com/std/3829236/astm-d4374-00.
[31] S. Parinyachet, Q. Leepowpanth, A study of residual cyanides and potential stabilities in tailings storage facility of gold mining operation, Appl. Environ. Res. 37 (1) (2015) 11–18. https://www.tci-thaijo.org/index.php/aer.
[32] Q.B. Tran, V. Khum-in, T. Phenrat, Assessing potential health impacts of cyanide-contaminated seepage in paddy field near a Gold Mine in Thailand: cyanide speciation and vapor intrusion modeling, Expo. Heal. 14 (2022) 459–473, https://doi.org/10.1007/s12403-022-00466-4.
[33] G. Desotelle, METHOD 14561CN free cyanide with pyridine - barbituric acid and photometry. https://www.sigmaaldrich.com/deepweb/assets/sigmaaldrich/product/documents/274/059/cyanide-spectroquant-114561-ww-method-1999.pdf?msockid=201e6274d71360fe0d037799d69161d2.
[34] J.W. O'Dell, Method 335.4: determination of total cyanide by semi-automated colorimetry, Environ. Monit. Syst. Lab. Off. Res. Dev. U.S. Environ. Prot. Agency 1 (1) (1993) 1–16.
[35] U.S. EPA, Definition and procedure for the determination of the method detection limit, United States Environ, Prot. Agency (2016) 1–8. https://www.law.cornell.edu/cfr/text/40/part-136/appendixB%5Cnhttp://www.epa.gov/region9/qa/pdfs/40cfr136_03.pdf.
[36] WHO, Cyanide in Drinking-water. Background Document for Development of WHO Guidelines for Drinking Water Quality, World Heal. Organ, 2009.
[37] Environmental Protection Agency, National Recommended Water Quality Criteria - Aquatic Life Criteria Table, USA Environ. Prot. Agency, 2016. https://www.epa.gov/wqc/national-recommended-water-quality-criteria-aquatic-life-criteria-table.
[38] Canadian Council of Ministers of the Environment (CCME), Canadian soil quality guidelines for the protection of environmental and human health, Can. Environ. Qual. Guidel. (1997).
[39] E.E. Kwaansa-Ansah, L.P. Amenorfe, E.K. Armah, F. Opoku, Human health risk assessment of cyanide levels in water and tuber crops from Kenyasi, a mining community in the Brong Ahafo Region of Ghana, Int. J. Food Contam. 4 (16) (2017), https://doi.org/10.1186/s40550-017-0061-y.
[40] L.C. Razanamahandry, H.A. Andrianisa, H. Karoui, K.M. Kouakou, H. Yacouba, Biodegradation of free cyanide by bacterial species isolated from cyanide-contaminated artisanal gold mining catchment area in Burkina Faso, Chemosphere 157 (2016) 71–78, https://doi.org/10.1016/j.chemosphere.2016.05.020.
[41] D. Stapper, K. Dales, P. Velasquez, S. Keane, Best management practices for cyanide use in the small-scale gold mining sector, PlanetGOLD Programme (Global Environment Facility and United Nations Environment Programme), 2021. https://www.planetgold.org/sites/default/files/CN%20Best%20Practices%20in%20ASGM_Final_Dec%2016%202021_0.pdf.
[42] D.B. Donato, O. Nichols, H. Possingham, M. Moore, P.F. Ricci, B.N. Noller, A critical review of the effects of gold cyanide-bearing tailings solutions on wildlife, Environ. Int. 33 (7) (2007) 974–984, https://doi.org/10.1016/j.envint.2007.04.007.
[43] T. Mudder, M.M. Botz, A. Smith, Chemistry and treatment of cyanidation wastes. http://dana6.free.fr/3%20060713%20English%20Compendium.pdf.
[44] K.B. Kouadio, E. Resongles, K.E. Ahoussi, Z. Ouattara, I. Konaté, N. Fayol, D. Borschneck, D. Baratoux, S. Delpoux, A. Domeau, M. Marie, K.A. Yao, O. Bruneel, Environmental contamination by metals, metalloids, and cyanides in the historic and active ASGM area of Kokumbo in Côte d'Ivoire, Environ. Sci. Pollut. Res 32 (23) (2025) 13699–13725, https://doi.org/10.1007/s11356-025-36403-6.
[45] N. Yurkevich, V. Olenchenko, S. Bortnikova, O. Saeva, T. Korneeva, Cyanides, arsenic, and noble metals in abandoned gold ore cyanidation tailings and surface waters in a permafrost region (Transbaikal Territory, Russia), Mine Water Environ 40 (2021) 943–955, https://doi.org/10.1007/s10230-021-00828-5.
[46] G.J. Zagury, K. Oudjehani, L. Deschênes, Characterization and availability of cyanide in solid mine tailings from gold extraction plants, Sci. Total Environ. 320 (2–3) (2004) 211–224, https://doi.org/10.1016/j.scitotenv.2003.08.012.
[47] S.D. Sagoe, S.J. Cobbina, R.W. Kazapoe, N.K. Bonso, J. Atopunga, Assessment of groundwater quality and exposure risks in a rural mining district of Ghana using multivariate and probabilistic approaches, Discov. Geosci. 3 (256) (2025), https://doi.org/10.1007/s44288-025-00355-8.

[48] B.G. Marshall, M.M. Veiga, H.A.M. da Silva, J.R.D. Guimarães, Cyanide Contamination of the Puyango-Tumbes River Caused by Artisanal Gold Mining in Portovelo-Zaruma, Ecuador, Curr. Environ. Heal. Reports 7 (3) (2020) 303–310, https://doi.org/10.1007/s40572-020-00276-3.

[49] ICMI. The International Cyanide Management Code, 2021. https://www.cyanidecode.org/wp-content/uploads/2021/06/01-The-Cyanide-Code-JUNE-2021.pdf.

[50] M.D. Welman-Purchase, J. Castillo, A. Gomez-arias, A. Matu, N. Hansen, First insight into the natural biodegradation of cyanide in a gold tailings environment enriched in cyanide compounds, Sci. Total Environ. 906 (2024) 167174, https://doi.org/10.1016/j.scitotenv.2023.167174.

[51] R. Bowell, Natural attenuation in the vadose zone: nature's gift to mine closure, Aust. Cent. Geomech. (2023), https://doi.org/10.36487/ACG_repo/2315_000.

[52] U.S. Environmental Protection Agency (EPA), National primary drinking water regulations, drink, Water Contam, http://water.epa.gov/drink/contaminants/index.cfm, 2013.

[53] H. Li, J. Peng, H. Long, S. Li, L. Zhang, Cleaner process: efficacy of chlorine in the recycling of gold from gold-containing tailings, J. Clean. Prod. (2020) 125066, https://doi.org/10.1016/j.jclepro.2020.125066.

[54] D.F. Caicedo, I.A.S. Brum, L.A.B. Buitrago, Photocatalytic degradation of ferricyanide as synthetic gold mining wastewater using TiO_2 assisted by H_2O_2, Min. Mineração 73 (1) (2020) 99–107, https://doi.org/10.1590/0370-44672019730042.

[55] N. Malmir, N.A. Fard, S. Aminzadeh, Z. Moghaddassi-jahromi, An overview of emerging cyanide bioremediation methods, Processes 10 (2022) 1724, https://doi.org/10.3390/pr10091724.

[56] F. Halet, A.R. Yeddou, A. Chergui, S. Chergui, B. Nadjemi, A. Ould-dris, Removal of cyanide from aqueous solutions by adsorption on activated carbon prepared from lignocellulosic by-products, J. Dispers. Sci. Technol. ISSN 36 (2015) 1736–1741, https://doi.org/10.1080/01932691.2015.1005311.

[57] A.A. Adnan, A. Ismayana, Removal of cyanide from an artificial wastewater in a constructed wetland system with Pistia stratiotes and C, Zizaniodes, IOP Conf. Ser. Earth Environ. Sci. 1063 (2022), https://doi.org/10.1088/1755-1315/1063/1/012018.

[58] Y. Wei, S. Chen, T. Ren, L. Chen, Y. Liu, J. Gao, Y. Li, Effectiveness and mechanism of cyanide remediation from contaminated soils using thermally activated persulfate, Chemosphere 292 (2022) 133463, https://doi.org/10.1016/j.chemosphere.2021.133463.